AIMS Mathematics

https://www.aimspress.com/journal/Math

AIMS Mathematics, 11(9): 27791–27825.
DOI: 10.3934/math.20261111
Received: 10 June 2026
Revised: 14 August 2026
Accepted: 18 August 2026
Published: 01 September 2026

Research article

Stability transitions induced by cross-transport mechanisms in a coupled reaction-advection-diffusion system

Ririn Setiyowati[1,2], Lina Aryati[1,*], Sumardi[1] and Nanang Susyanto[1]

[1] Department of Mathematics, Faculty of Mathematics and Natural Sciences, Universitas Gadjah Mada, Yogyakarta, Indonesia

[2] Department of Mathematics, Faculty of Mathematics and Natural Sciences, Universitas Sebelas Maret, Surakarta, Indonesia

* **Correspondence:** Email: lina@ugm.ac.id; Tel: +6281328786078.

Abstract: The complexity of spatial interactions in nature often gives rise to emergent patterns that cannot be explained by local dynamics alone. An investigation is conducted into how cross-diffusion and cross-advection govern the stability of general reaction-advection-diffusion system on an infinite spatial domain. The analysis is formulated for nonlinear reaction terms using the reaction Jacobian, diffusion matrix, and advection matrix. By applying normal-mode decomposition, the Routh-Hurwitz criterion for complex characteristic polynomials, and the critical neutral curve method, we derive stability conditions and identify instability boundaries in parameter space. The results show that a constant equilibrium stable under the local reaction dynamics remains stable under self-diffusion and self-advection. In the baseline kinetic setting, cross-advection alone also preserves stability when cross-diffusion is absent. In contrast, cross-diffusion can destabilize the equilibrium and interact with cross-advection to reshape the unstable region. Under different kinetic-sign conditions, asymmetric cross-advection may induce instability even in the absence of cross-diffusion. The predator-prey application supports these findings, as weak transport interactions preserve homogeneous coexistence while sufficiently strong cross-transport generates unstable spatial modes and visible spatiotemporal patterns. Cross-diffusion initiates spatial organization through density-gradient responses between prey and predator. In contrast, cross-advection modifies the direction, intensity, and propagation of the resulting patterns through directed movement such as prey avoidance and predator pursuit. These results provide a systematic framework for detecting cross-transport-induced instability and explaining the transition from homogeneous coexistence to pattern-forming dynamics.

Keywords: cross-diffusion; cross-advection; transport-induced instability; neutral curve; Routh-Hurwitz criterion; reaction-advection-diffusion system; predator-prey patterns
Mathematics Subject Classification: 35N05, 35E20

1. Introduction

Reaction-advection-diffusion (RAD) systems constitute a fundamental framework for modeling spatiotemporal phenomena in ecology, chemistry, biology, epidemiology, environmental science, and reaction engineering [10, 24, 45]. They have been extensively employed to describe predator-prey interactions [4, 18, 40, 44], population dispersal [29], chemical reactor dynamics [8, 13], infectious disease transmission [36, 39], and pollutant transport processes [11, 30]. Through the interaction of local reaction kinetics, diffusion, and advection, RAD models are capable of exhibiting equilibrium stabilization, diffusion-driven destabilization, bifurcation, chaotic dynamics, traveling waves, and spatial pattern formation [1, 24, 31, 41, 42]. However, most classical formulations are based only on self-diffusion and self-advection so that each component responds exclusively to its own gradient or prescribed flow. This assumption may be too restrictive for many interacting systems in which one component moves in response to another, thereby requiring the inclusion of cross-diffusion and cross-advection terms [23, 33, 35, 46].

The classical RAD models have been significantly extended by adding cross-diffusion and cross-advection, which describe transport processes due to interactions between the components of the system. Cross-diffusion refers to the movement caused by the gradient of another population or concentration, including prey-taxis, avoidance, aggregation, and exclusion effects [19, 23, 35], while cross-advection is the directed transport by other populations, environmental carriers, or external flow-mediated interactions, such as host-mediated dispersal or component-dependent drift [5, 26, 36]. Such cross-interaction terms can be primary processes that change the stability landscape of constant equilibrium solutions, rather than auxiliary refinements of the transport operator [19, 26, 33]. Hence, models that do not include cross-diffusion and cross-advection may miss important instability mechanisms and underestimate the onset and richness of nonuniform spatiotemporal structures observed in ecological, epidemiological, and chemical systems [5, 19, 26, 27, 36].

Cross-effects have been found to strongly affect traveling waves, oscillating fronts, and pattern–forming dynamics in previous studies [41, 42]. However, the analytical characterization of their significance in generalized RAD systems has remained limited. Many existing investigations either neglect advection, exclude cross-interactions, or rely primarily on numerical observations rather than complete analytical criteria [6, 13, 20, 28, 34]. As a result, the precise mechanism by which cross-diffusion and cross-advection reshape stability regions, modify neutral stability boundaries, and generate distinct instability frontiers remains poorly understood. This gap is particularly important because cross-interactions may destabilize constant equilibrium solutions even when the corresponding reaction system is locally stable and self-transport alone cannot trigger instability under standard assumptions.

Motivated by this gap, this study develops a general analytical framework for examining stability and instability induced by cross-diffusion and cross-advection in a coupled reaction-advection-diffusion system on an infinite spatial domain. Hereafter, the reaction-advection-diffusion system incorporating cross-diffusion and cross-advection is referred to as the RADCDCA system. The analysis is formulated in terms of the reaction Jacobian, diffusion matrix, and advection matrix, which combines normal-mode decomposition with the Routh-Hurwitz criterion for complex characteristic polynomials and the critical neutral curve method [5, 38]. Within this setting, explicit stability conditions and instability boundaries are derived to determine when a constant equilibrium solution remains stable and when it loses stability through transport-induced mechanisms. The results clarify how cross-diffusion can initiate destabilization, how cross-advection can either preserve stability or reshape the unstable region, and under which kinetic sign structures asymmetric cross-advection alone may generate instability even in the absence of cross-diffusion. As a concrete illustration, a predator-prey model is employed to demonstrate how the general stability framework can be used to assess the impact of cross-diffusion and cross-advection on the robustness of a constant coexistence solution and on the possible emergence of spatially structured dynamics in the ecological RADCDCA system.

Building on this framework, the main contribution of this study lies in clarifying the distinct roles of self-transport and cross-transport mechanisms in the stability structure of the general RADCDCA system, by explicitly separating the effects of self-diffusion and self-advection from those of cross-diffusion and cross-advection and identifying how each class of transport terms enters the dispersion relation and shapes instability boundaries in parameter space. The remainder of this paper is organized as follows. Section 2 presents the generalized RADCDCA system on an infinite spatial domain and determines their constant equilibrium solutions. Section 3 develops the linear stability analysis and derives the corresponding Routh-Hurwitz stability criteria. Section 4 examines the instability regions in the parameter space induced by cross-diffusion and cross-advection mechanisms, analyzed through the critical neutral curve method. Section 5 applies the theoretical results to a predator-prey model and examines their consistency with numerically observed spatiotemporal dynamics. Finally, Section 6 concludes the paper.

2. RADCDCA system on an infinite spatial domain

In the following, we consider the general formulation of a coupled RADCDCA system on an infinite spatial domain

$$
\begin{aligned}
\frac{\partial u}{\partial t} &= d_{11}\frac{\partial^2 u}{\partial x^2} + d_{12}\frac{\partial^2 v}{\partial x^2} - a_{11}\frac{\partial u}{\partial x} - a_{12}\frac{\partial v}{\partial x} + F(u,v), \quad x \in \mathbb{R}, t \geq 0,\\
\frac{\partial v}{\partial t} &= d_{21}\frac{\partial^2 u}{\partial x^2} + d_{22}\frac{\partial^2 v}{\partial x^2} - a_{21}\frac{\partial u}{\partial x} - a_{22}\frac{\partial v}{\partial x} + G(u,v), \quad x \in \mathbb{R}, t \geq 0,\\
u(x,0) &= u_0(x), \quad v(x,0) = v_0(x), \quad x \in \mathbb{R},
\end{aligned}
\tag{2.1}
$$

where $\mathbb{R} = (-\infty, \infty)$. Here, we assume that all diffusion coefficients $d_{ij} > 0$ and all advection coefficients $a_{ij} > 0$ for $i, j = 1, 2$. Self-diffusion connects the flux of a component with its own concentration gradient, while cross-diffusion connects the flux of the component with the concentration gradients of other components [25]. Self-advection refers to the movement of a substance due to its own concentration gradient, while cross-advection refers to the movement of one substance due to the concentration gradient of another [41]. Based on basic thermodynamics and Fick's rule of diffusion, we assume that $d_{11}d_{22} - d_{12}d_{21} > 0$ and that the self-diffusion coefficient is always larger than the cross-diffusion coefficient. These conditions ensure normal ellipticity of the diffusion operator and describe a physically relevant regime in which self-diffusion dominates repulsive cross-diffusion. Both self-advection and cross-advection are predicated on the idea that $a_{11}a_{22} - a_{12}a_{21} > 0$. This is due to the fact that in a particular system, self-advection predominates over cross-advection. The functions $F(u, v)$ and $G(u, v)$ in system (2.1) are called the reaction functions.

One approach to understanding the behavior of the system solutions is to examine solutions that are independent of both time and space, hereafter referred to as constant equilibrium solutions. Let (u_e, v_e)

be a constant equilibrium solution for system (2.1) in general. Clearly, (u_e, v_e) is also an equilibrium solution for the system of ordinary differential equations (ODEs)

$$\begin{aligned} \frac{du}{dt} &= F(u, v), \\ \frac{dv}{dt} &= G(u, v). \end{aligned} \tag{2.2}$$

For simplicity, we denote by F_u, F_v, G_u, and G_v the first-order partial derivatives of F and G at the constant equilibrium solution (u_e, v_e). The constant equilibrium (u_e, v_e) of the ODE system (2.2) is asymptotically stable if and only if the Jacobian matrix

$$J = \begin{pmatrix} F_u & F_v \\ G_u & G_v \end{pmatrix}$$

satisfies the Routh-Hurwitz criterion (see Theorem 3.4.71 in [12]), namely

$$Tr(J) = F_u + G_v < 0, \quad \det(J) = F_u G_v - F_v G_u > 0. \tag{2.3}$$

Equivalently, all eigenvalues of J have negative real parts. Under the assumption $F_v G_u < 0$, which implies antagonistic cross interactions between the two components, the sign configurations of the Jacobian entries compatible with condition (2.3) reduce to the following three cases:

(A) $F_u < 0$, $G_v < 0$, and $F_v G_u < 0$,
(B) $F_u < 0$, $G_v > 0$, and $F_v G_u < 0$,
(C) $F_u > 0$, $G_v < 0$, and $F_v G_u < 0$.

Condition (A) was investigated by [14, 43] in a predator-prey model with $F(u, v) = u(a - u - m_1 v)$ and $G(u, v) = v(b + m_2 u - v)$. Conditions (B) and (C) are found in the activator and inhibitor model in a biological system [2, 7, 9, 17, 24].

3. Linear stability analysis

More formally, we analyze the local stability of the nonlinear RADCDCA system (2.1). We consider a small pertubation $(\hat{u}, \hat{v})$ of the constant equilibrium solution (u_e, v_e) and substitute

$$u = u_e + \hat{u}, \quad v = v_e + \hat{v}, \tag{3.1}$$

into system (2.1). The linearization of functions $F(u, v)$ and $G(u, v)$ at the constant equilibrium solution (u_e, v_e) is approximated using Taylor series. Thus, we obtain the linearization of system (2.1) as

$$\begin{aligned} \frac{\partial \mathbf{w}}{\partial t} &= D\frac{\partial^2 \mathbf{w}}{\partial x^2} - A\frac{\partial \mathbf{w}}{\partial x} + J\mathbf{w}, \\ \mathbf{w}(x, 0) &= \mathbf{w}_0(x), \end{aligned} \tag{3.2}$$

where

$$\mathbf{w} = \begin{pmatrix} \hat{u} \\ \hat{v} \end{pmatrix}, \quad \frac{\partial \mathbf{w}}{\partial t} = \begin{pmatrix} \frac{\partial \hat{u}}{\partial t} \\ \frac{\partial \hat{v}}{\partial t} \end{pmatrix}, \frac{\partial^2 \mathbf{w}}{\partial x^2} = \begin{pmatrix} \frac{\partial^2 \hat{u}}{\partial x^2} \\ \frac{\partial^2 \hat{v}}{\partial x^2} \end{pmatrix}, \quad \frac{\partial \mathbf{w}}{\partial x} = \begin{pmatrix} \frac{\partial \hat{u}}{\partial x} \\ \frac{\partial \hat{v}}{\partial x} \end{pmatrix},$$

$$D = \begin{pmatrix} d_{11} & d_{12} \\ d_{21} & d_{22} \end{pmatrix}, \quad A = \begin{pmatrix} a_{11} & a_{12} \\ a_{21} & a_{22} \end{pmatrix}, \quad J = \begin{pmatrix} F_u & F_v \\ G_u & G_v \end{pmatrix},$$

and

$$\mathbf{w}_0(x) = \begin{pmatrix} u_0(x) - u_e \\ v_0(x) - v_e \end{pmatrix}.$$

One can characterize the local behavior of $\mathbf{w}(x,t)$ through its spatial Fourier modes $\mathbf{W}(k,t)$ defined over the domain $x \in \mathbb{R}$. In particular, let $\mathbf{W}(k,t)$ be the Fourier coefficients of $\mathbf{w}(x,t)$ satisfying

$$\mathbf{w}(x,t) = \frac{1}{2\pi} \int_{k\in\mathbb{R}} \mathbf{W}(k,t) e^{ikx} dk, \tag{3.3}$$

where $\mathbb{R}$ is the set of real numbers, k denotes the wavenumber, and $i = \sqrt{-1}$. The wavenumber k is a positive real number.

By using a Fourier transform for an infinite domain, we obtain the linear system

$$\frac{\partial \mathbf{W}}{\partial t} = (-Dk^2 - ikA + J)\mathbf{W}(k,t). \tag{3.4}$$

The following theorem provides the solution of the linear system.

Theorem 3.1. *Given a linear system*

$$\begin{aligned} \frac{d\boldsymbol{W}}{dt} &= M_k \boldsymbol{W}, \\ \boldsymbol{W}(0) &= \boldsymbol{W}_0, \end{aligned} \tag{3.5}$$

where $\boldsymbol{W}_0, \boldsymbol{W} \in \mathbb{R}^2$ and $M_k = -Dk^2 - ikA + J$ is a 2×2 matrix. Then, system (3.5) has a unique solution,

$$\boldsymbol{W}(t) = \boldsymbol{W}_0 e^{M_k t}, k \in \mathbb{R}^+. \tag{3.6}$$

Proof. Equation (3.4) is an ODE system. For a fixed value of k, Equation (3.4) is rewritten as

$$\frac{d\mathbf{W}}{dt} = (-Dk^2 - ikA + J)\mathbf{W}, \tag{3.7}$$

with the initial condition

$$\mathbf{W}(0) = \mathbf{W}_0, \tag{3.8}$$

The solution of system (3.7) is

$$\mathbf{W}(t) = \mathbf{K} e^{(-Dk^2 - ikA + J)t}, \tag{3.9}$$

with arbitary constant $\mathbf{K}$. Considering the initial value problems (3.8), we obtain

$$\mathbf{W}_0 = \mathbf{K}.$$

In other words, the initial value problems (3.7) and (3.8) have a unique solution, namely

$$\mathbf{W}(t) = \mathbf{W}_0 e^{M_k t}$$

where $M_k = -Dk^2 - ikA + J$ and $k \in \mathbb{R}^+$. □

For each fixed k, Equation (3.4) represents a time-dependent system of ODEs with complex coefficients. We begin the stability analysis by linearizing the system, as stated in the following lemma.

Lemma 3.2. *Consider the linearization of the RADCDCA system (3.2) and the characteristic equation*

$$|\lambda I - (-Dk^2 - ikA + J)| = 0. \tag{3.10}$$

1. *The constant equilibrium solution of system (3.2) is asymptotically stable if all roots of the characteristic polynomial (3.10) have a negative real part for every positive real number k.*
2. *The constant equilibrium solution of system (3.2) is unstable if there exists a root of the characteristic polynomial (3.10) with a positive real part for some positive real number k.*

In Lemma 3.2, we emphasize that verifying the stability criteria requires solving an infinite sequence of characteristic equations with complex coefficients as given in (3.10). Explicit analytical conditions can generally be derived only in certain special cases. To analyze the linear stability of (u_e, v_e), we introduce the matrix

$$M_k = \begin{pmatrix} -d_{11}k^2 - ia_{11}k + F_u & -d_{12}k^2 - ia_{12}k + F_v \\ -d_{21}k^2 - ia_{21}k + G_u & -d_{22}k^2 - ia_{22}k + G_v \end{pmatrix}. \tag{3.11}$$

The characteristic equation of the matrix M_k is given by

$$\lambda^2 - (p_1 + iq_1)\lambda + (p_0 + iq_0) = 0, \tag{3.12}$$

where

$$p_1 = \tau_J - \tau_D k^2, \quad q_1 = -\tau_A k, \quad p_0 = \Lambda_J - (\Lambda_A + \tau_{DJ})k^2 + \Lambda_D k^4, \quad q_0 = \tau_{AD}k^3 - \tau_{AJ}k, \tag{3.13}$$

with

$$\begin{aligned} \tau_J = F_u + G_v, \tau_A = a_{11} + a_{22}, \tau_D = d_{11} + d_{22}, \Lambda_J = F_u G_v - F_v G_u, \\ \Lambda_A = a_{11}a_{22} - a_{12}a_{21}, \Lambda_D = d_{11}d_{22} - d_{12}d_{21}, \tau_{DJ} = d_{22}F_u - d_{21}F_v - d_{12}G_u + d_{11}G_v, \\ \tau_{AJ} = a_{22}F_u - a_{21}F_v - a_{12}G_u + a_{11}G_v, \tau_{AD} = a_{22}d_{11} - a_{21}d_{12} - a_{12}d_{21} + a_{11}d_{22}. \end{aligned} \tag{3.14}$$

We investigate the linear stability of the constant equilibrium solution (u_e, v_e) by means of the Routh–Hurwitz criterion for complex polynomials (see Theorem 3.4.68 in [12]). We start by separating the real and imaginary components of the coefficients of the characteristic equation (3.12) and obtain $\bar{p}_R(\lambda) = -\lambda^2 + q_1\lambda + p_0$ and $\bar{p}_I(\lambda) = -p_1\lambda + q_0$. Second, we generate a 4×4 Hurwitz matrix using real and imaginary components of the characteristic equation (3.12), which is

$$H = \begin{pmatrix} 0 & -p_1 & q_0 & 0 \\ -1 & q_1 & p_0 & 0 \\ 0 & 0 & -p_1 & q_0 \\ 0 & -1 & q_1 & p_0 \end{pmatrix}. \tag{3.15}$$

Next, we define the even-order principal minors of the matrix H,

$$\Delta_1(k) = \begin{vmatrix} 0 & -p_1 \\ -1 & q_1 \end{vmatrix} = -p_1, \tag{3.16}$$

$$\Delta_2(k) = \begin{vmatrix} 0 & -p_1 & q_0 & 0 \\ -1 & q_1 & p_0 & 0 \\ 0 & 0 & -p_1 & q_0 \\ 0 & -1 & q_1 & p_0 \end{vmatrix} = p_0 p_1^2 + p_1 q_1 q_0 - q_0^2. \tag{3.17}$$

According to the Routh-Hurwitz criterion for polynomials with complex coefficients, all roots of the characteristic equation (3.12) have a negative real part for every positive real number k if and only if the even-order principal minors of the matrix H are positive. Based on the principal minors (3.16) and (3.17), $\Delta_1(k) > 0$ if $p_1 < 0$ and $\Delta_2(k) > 0$ if $p_0 p_1^2 + p_1 q_1 q_0 - q_0^2 > 0$. Therefore, we can conclude that all roots of the characteristic equation (3.12) have $Re(\lambda_{1,2}) < 0$ if and only if they satisfy the condition

$$p_1 < 0 \text{ and } p_1^2 p_0 + p_1 q_1 q_0 - q_0^2 > 0. \tag{3.18}$$

Based on the Routh-Hurwitz criterion for the characteristic equations (3.12), we obtain the results presented in the following lemma.

Lemma 3.3. *Given characteristic equations with complex coefficients (3.12). Then, we have the following results:*

1. *If $p_1 < 0$ and $p_1^2 p_0 + p_1 q_1 q_0 - q_0^2 > 0$, then all roots of the characteristic equation (3.12) have negative real parts for all k.*
2. *If $p_1^2 p_0 + p_1 q_1 q_0 - q_0^2 = 0$, then there is a root of the characteristic equation (3.12) whose real part is zero for some k.*
3. *If $p_1 \geq 0$ or $p_1^2 p_0 + p_1 q_1 q_0 - q_0^2 \leq 0$, then there exists root of the characteristic equation (3.12) that has positive real part for some k.*

Now, we use Lemma 3.3 to analyze the linear stability of the constant equilibrium solution (u_e, v_e) with p_0, p_1, q_0, and q_1 in (3.13) and (3.14). Based on the assumption that $\tau_D > 0$, the condition $p_1 = \tau_J - \tau_D k^2 < 0$ holds whenever $\tau_J < 0$. The second condition for the constant equilibrium solution to be asymptotically stable is $p_1^2 p_0 + p_1 q_1 q_0 - q_0^2 > 0$ for $p_1 < 0$.

Lemma 3.4. *For $p_1 < 0$, inequality $p_1^2 p_0 + p_1 q_1 q_0 - q_0^2 > 0$ has a solution $q_0 \in \mathbb{R}$ if and only if $q_1^2 + 4p_0 > 0$.*

Proof. For $p_1 < 0$, the term $p_1^2 p_0 + p_1 q_1 q_0 - q_0^2$ can be written as a quadratic function of q_0, namely $f(q_0) = -q_0^2 + p_1 q_1 q_0 + p_1^2 p_0$. The coefficient q_0^2 is -1, so the curve $f(q_0)$ is a parabola that opens downward with maximum value $f(q_0^*) = \frac{p_1^2}{4}(q_1^2 + 4p_0)$ at $q_0^* = \frac{p_1 q_1}{2}$. If there is q_0 with $f(q_0) > 0$, then automatically $f(q_0^*) > 0$. Since $p_1^2 > 0$, we must have $q_1^2 + 4p_0 > 0$. If $q_1^2 + 4p_0 > 0$, then $f(q_0^*) > 0$. Since $f(q_0)$ is continuous and reaches a positive maximum at q_0^*, there exists an open interval around q_0^* with $f(q_0) > 0$. The equation $f(q_0) = 0$ has two solutions, namely

$$q_0 = \frac{p_1 q_1 \pm \sqrt{p_1^2 (q_1^2 + 4p_0)}}{2}.$$

Since $p_1 < 0$, then the q_0 that satisfies inequality $f(q_0) > 0$ lies between q_0^- and q_0^+ with

$$q_0^- = \frac{p_1 (q_1 + \sqrt{q_1^2 + 4p_0})}{2} \text{ and } q_0^+ = \frac{p_1 (q_1 - \sqrt{q_1^2 + 4p_0})}{2}.$$

□

Now, we consider p_1, p_0, q_1, and q_0 in (3.13). Since $\tau_D > 0$, then the condition $p_1 < 0$ is satisfied for $\tau_J < 0$. From Lemma 3.4, the necessary and sufficient condition for the inequality $p_1^2 p_0 + p_1 q_1 q_0 - q_0^2 > 0$ is $q_1^2 + 4p_0 > 0$. The condition $q_1^2 + 4p_0 > 0$ can be written in the form

$$\Lambda_D k^4 - (\Lambda_A - \frac{1}{4}\tau_A^2 + \tau_{DJ})k^2 + \Lambda_J > 0. \tag{3.19}$$

Lemma 3.5. *Assume that $\Lambda_D > 0$ and $\Lambda_J > 0$ hold. Inequality (3.19) holds for all $k \in \mathbb{R}^+$ if and only if one of the following condition is satisfied:*

1. $\Lambda_A - \frac{1}{4}\tau_A^2 + \tau_{DJ} < 0$, *or*
2. $\Lambda_A - \frac{1}{4}\tau_A^2 + \tau_{DJ} > 0$ *and* $(\Lambda_A - \frac{1}{4}\tau_A^2 + \tau_{DJ})^2 - 4\Lambda_D\Lambda_J < 0$.

Proof. By substituting $\kappa = k^2 > 0$, Inequality (3.19) can be reduced to the quadratic inequality

$$f(\kappa) = \Lambda_D \kappa^2 - (\Lambda_A - \frac{1}{4}\tau_A^2 + \tau_{DJ})\kappa + \Lambda_J > 0$$

for all $\kappa \geq 0$. Since $\Lambda_D > 0$ and $\Lambda_J > 0$, the parabola $f(\kappa)$ opens upward.

1. Since $\Lambda_D > 0$ and $\Lambda_J > 0$, the product of the roots $\kappa_1\kappa_2 = \Lambda_J/\Lambda_D > 0$, and it follows that both roots of the equation $f(\kappa) = 0$ have the same sign. When $\Lambda_A - \frac{1}{4}\tau_A^2 + \tau_{DJ} < 0$, the sum of the roots $\kappa_1 + \kappa_2 = (\Lambda_A - \frac{1}{4}\tau_A^2 + \tau_{DJ})/\Lambda_D$ is negative. Therefore, both roots must be negative. Thus, the curve $f(\kappa)$ does not intersect the κ-axis, and $f(\kappa) > 0$ for all $\kappa \geq 0$.
2. If $\Lambda_A - \frac{1}{4}\tau_A^2 + \tau_{DJ} < 0$, then the minimum point occurs at $\kappa^* = \frac{\Lambda_A - \frac{1}{4}\tau_A^2 + \tau_{DJ}}{2\Lambda_D} < 0$ provided $\Lambda_D > 0$. Thus, the minimum of $f(\kappa)$ lies to the left of $\kappa = 0$. Consequently, the function $f(\kappa)$ is strictly increasing for $\kappa \geq 0$. In other words, we obtain $\min_{\kappa \geq 0} f(\kappa) = \Lambda_J > 0$. For $\Lambda_A - \frac{1}{4}\tau_A^2 + \tau_{DJ} > 0$, the parabola $f(\kappa)$ reaches its minimum

$$f(\kappa^*) = -(\Lambda_A - \frac{1}{4}\tau_A^2 + \tau_{DJ})^2 + 4\Lambda_D\Lambda_J$$

at $\kappa^* = \frac{\Lambda_A - \frac{1}{4}\tau_A^2 + \tau_{DJ}}{2\Lambda_D}$. Since $\Lambda_A - \frac{1}{4}\tau_A^2 + \tau_{DJ} > 0$ and $(\Lambda_A - \frac{1}{4}\tau_A^2 + \tau_{DJ})^2 - 4\Lambda_D\Lambda_J < 0$, then $\kappa^* > 0$ and $f(\kappa^*) > 0$.

□

According to Lemma 3.2-3.5, we summarize the results of this linear stability analysis of the constant equilibrium solution in the following theorem.

Theorem 3.6. *We have matrices D, A, J defined as*

$$D = \begin{pmatrix} d_{11} & d_{12} \\ d_{21} & d_{22} \end{pmatrix}, \quad A = \begin{pmatrix} a_{11} & a_{12} \\ a_{21} & a_{22} \end{pmatrix}, J = \begin{pmatrix} F_u & F_v \\ G_u & G_v \end{pmatrix}.$$

where $d_{ij} > 0$, $a_{ij} > 0$ for $i, j = 1, 2$, and p_0, p_1, q_0, q_1 in (3.13) and (3.14). The constant equilibrium solution (u_e, v_e) of the RADCDCA system (2.1) is asymptotically stable if and only if

$$\tau_J < 0, \quad \Lambda_J > 0, \tag{3.20}$$

and one of the conditions

$$\Lambda_A - \frac{1}{4}\tau_A^2 + \tau_{DJ} < 0, \tag{3.21}$$

or

$$\Lambda_A - \frac{1}{4}\tau_A^2 + \tau_{DJ} > 0, \tag{3.22}$$

$$(\Lambda_A - \frac{1}{4}\tau_A^2 + \tau_{DJ})^2 - 4\Lambda_D\Lambda_J < 0 \tag{3.23}$$

is satisfied for every positive real number k.

Theorem 3.6 shows that a constant equilibrium solution that is stable for the ODE system remains stable after diffusion and advection are introduced, provided that conditions (3.20)-(3.21) or (3.22)-(3.23) with $\tau_J < 0$ and $\Lambda_J > 0$ hold. When $k = 0$, these conditions reduce to the linear stability condition of the ODE system (2.2), whereas instability may emerge only if they fail for some nonzero wavenumber. Moreover, we examine the particular case of system (2.1) in the absence of cross-diffusion ($d_{12} = d_{21} = 0$) and cross-advection ($a_{12} = a_{21} = 0$).

Corollary 3.7 (RD system)**.** *If $d_{12} = d_{21} = 0$, $a_{11} = a_{22} = a_{12} = a_{21} = 0$, and condition (A) holds, then the constant equilibrium solution (u_e, v_e) of system (2.1) is asymptotically stable.*

Proof. Since $F_u < 0$, $G_v < 0$, and $F_vG_u < 0$, then $\tau_J < 0$ and $\Lambda_J > 0$. Next, we substitute $d_{12} = d_{21} = 0$ and $a_{11} = a_{22} = a_{12} = a_{21} = 0$ into $\Lambda_A - \frac{1}{4}\tau_A^2 + \tau_{DJ}$ and obtain $d_{11}F_u + d_{22}G_v$. Based on the assumption, we get $d_{11}F_u + d_{22}G_v < 0$. So, the condition (3.20) is satisfied. According to Theorem 3.6, the constant equilibrium solution is asymptotically stable. □

Corollary 3.8 (RAD system)**.** *If $d_{12} = d_{21} = 0$, $a_{12} = a_{21} = 0$, and condition (A) holds, then the constant equilibrium solution (u_e, v_e) of system (2.1) is asymptotically stable.*

Proof. Using the same method as in the Corollary 3.7, we obtain $\tau_J < 0$, $\Lambda_J > 0$, and

$$\Lambda_A - \frac{1}{4}\tau_A^2 + \tau_{DJ} = -\frac{1}{4}(a_{11} - a_{22})^2 + d_{11}F_u + d_{22}G_v < 0$$

which satisfies condition (3.20). From Theorem 3.6, the constant equilibrium solution (u_e, v_e) of system (2.1) is asymptotically stable. □

After deriving the conditions that guarantee the asymptotic stability of the constant equilibrium solution, it is natural to consider the complementary case in which these conditions do not hold. Viewed in this way, Theorem 3.6 also identifies the threshold separating stability from instability, and the following result describes the corresponding instability of the RADCDCA system.

4. Instability induced by cross-diffusion and cross-advection

In the RADCDCA system (2.1), a transport-driven instability mechanism arises when a constant equilibrium solution remains asymptotically stable in the absence of diffusion and advection, yet loses its stability once transport effects are incorporated into the system. To investigate this transition systematically, we examine the respective roles of self-diffusion, self-advection, cross-diffusion, and cross-advection within the general RAD framework. As established in Lemma 3.3, the real parts of the eigenvalues $\mathrm{Re}(\lambda_{1,2}(k))$ depend on the algebraic expression $p_1^2 p_0 + p_1 q_1 q_0 - q_0^2$, whose sign cannot be determined directly owing to its intricate dependence on the model parameters and the wavenumber k. Consequently, a more systematic spectral criterion is required to detect the onset of instability and to characterize the precise conditions under which it occurs. To this end, we employ the critical neutral curve method, supported by the following zero-point theorem introduced in [24].

Lemma 4.1. *[24] The requirement that* $\mathrm{Re}(\lambda_{1,2}(k)) > 0$ *for some wavenumber k is equivalent to the existence of at least one solution of the equation* $\mathrm{Re}(\lambda_{1,2}(k)) = 0$ *with respect to k. Conversely, if equation* $\mathrm{Re}(\lambda_{1,2}(k)) = 0$ *admits no solutions, then* $\mathrm{Re}(\lambda_{1,2}(k)) < 0$ *holds for all k.*

By virtue of Lemma 4.1, determining whether instability occurs reduces to investigating the solvability of $\mathrm{Re}(\lambda_{1,2}(k)) = 0$ with respect to k. Applying Lemma 3.3 and carrying out straightforward calculations, this condition yields the following critical equation:

$$p_1^2 p_0 = q_0^2 - p_1 q_1 q_0. \tag{4.1}$$

Equation (4.1) defines the neutral curve that separates the stability and instability regions in parameter space. If Equation (4.1) admits at least one real solution with respect to k, then there exists a wavenumber for which $\mathrm{Re}(\lambda_{1,2}(k)) > 0$, and the constant equilibrium is therefore unstable. Conversely, if Equation (4.1) has no real solution, the equilibrium remains asymptotically stable for all k. The resulting neutral curves provide a rigorous framework for delineating the parameter regimes in which the constant equilibrium transitions from asymptotically stable to unstable.

To analyze the instability mechanism in a structured and progressive manner, we organize the investigation into four cases of increasing generality. We begin by examining whether self-diffusion and self-advection alone are sufficient to induce instability, and subsequently introduce cross-diffusion and cross-advection to assess their individual and combined contributions. Each case is analyzed by determining whether the associated neutral curve equation admits real solutions, thereby identifying the transport mechanism responsible for destabilizing the homogeneous equilibrium.

We first examine the stability properties of the RAD system under the assumption that cross-diffusion and cross-advection effects are absent, that is, $d_{12} = d_{21} = 0$ and $a_{12} = a_{21} = 0$. Under these conditions, the RAD system reduces to the following form:

$$\begin{aligned}
&\frac{\partial u}{\partial t} = d_{11}\frac{\partial^2 u}{\partial x^2} - a_{11}\frac{\partial u}{\partial x} + F(u,v), \quad x \in \mathbb{R}, t \geq 0,\\
&\frac{\partial v}{\partial t} = d_{22}\frac{\partial^2 v}{\partial x^2} - a_{22}\frac{\partial v}{\partial x} + G(u,v), \quad x \in \mathbb{R}, t \geq 0,\\
&u(x,0) = u_0(x), \quad v(x,0) = v_0(x), \quad x \in \mathbb{R}.
\end{aligned} \tag{4.2}$$

This case serves as a necessary baseline. Should self-diffusion and self-advection prove insufficient to destabilize the constant equilibrium solution (u_e, v_e), any instability observed in subsequent cases must be attributed exclusively to the cross-transport terms. The following theorem establishes the stability properties of the RAD system (4.2).

Theorem 4.2. *If* $d_{12} = d_{21} = a_{12} = a_{21} = 0$ *and condition (A) hold, then the constant equilibrium solution* (u_e, v_e) *of RAD system (4.2) is asymptotically stable. That is, self-diffusion and self-advection alone do not induce linear instability in the RAD system.*

Proof. To analyze the linear stability of the RAD system (4.2), we use Lemma 4.1 and Equation (4.1). By (4.1), we evaluate

$$p_1^2 p_0 = (-(d_{11}+d_{22})k^2+(F_u+G_v))^2(F_uG_v-F_vG_u-(a_{11}a_{22}-a_{12}a_{21}+d_{11}G_v+d_{22}F_u)k^2+d_{11}d_{22}k^4) \quad (4.3)$$

and

$$\begin{aligned} q_0^2 - p_1q_1q_0 =&((a_{11}F_v + a_{22}G_u)k - (a_{11}d_{22} + a_{22}d_{11})k^3)^2 - (- (d_{11} + d_{22})k^2 + (F_u + G_v)) \\ &(a_{11} + a_{22})k((a_{11}F_v + a_{22}G_u)k - (a_{11}d_{22} + a_{22}d_{11})k^3). \end{aligned} \quad (4.4)$$

Next, we evaluate (4.3) and (4.4) by adding the term $(a_{11} + a_{22})k^2(- (d_{11} + d_{22})k^2 + (F_u + G_v))^2$ to both equations and substitute them into (4.1), so that we obtain

$$\begin{aligned} (F_u + G_v - (d_{11} + d_{22})k^2)^2(-F_vG_u + (F_u - d_{11}k^2)(G_v - d_{22}k^2)) =&k^2(a_{11} - a_{22})^2(F_u - d_{11}k^2) \\ &(-G_v + d_{22}k^2). \end{aligned}$$

Since $F_u < 0$, $G_v < 0$, and $F_vG_u < 0$, then $(F_u + G_v - (d_{11} + d_{22})k^2)^2(-F_vG_u + (F_u - d_{11}k^2)(G_v - d_{22}k^2)) > 0$ and $k^2(a_{11} - a_{22})^2(F_u - d_{11}k^2)(-G_v + d_{22}k^2) < 0$, which contradicts (4.1). According to Lemma 4.1, since the equation $Re(\lambda_{1,2}) = 0$ has no solution, then $Re(\lambda_{1,2}) < 0$ for all k. Referring to Lemma 3.3, the analysis demonstrates that the constant equilibrium solution of the RAD system (4.2) is asymptotically stable. In other words, self-diffusion and self-advection in the RAD system does not induce instability. □

The conclusion of Theorem 4.2 is illustrated by the dispersion relations in Figure 1.

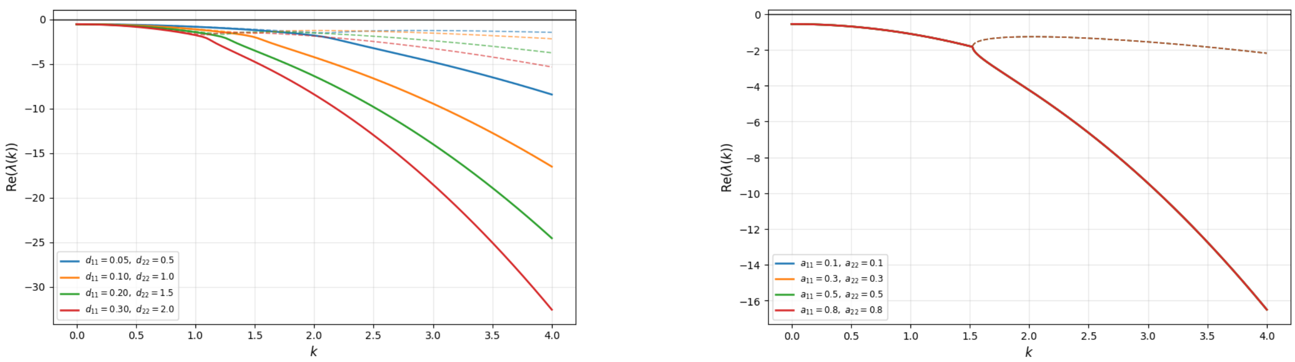

(a) Variation d_{11}, d_{22} with $a_{11} = 0.2, a_{22} = 0.3$ **(b)** Variation a_{11}, a_{22} with $d_{11} = 0.1, d_{22} = 1$

Figure 1. Plot of $\text{Re}(\lambda_{1,2}(k))$ versus k with $F_u = -0.5$, $G_v = -0.6$, $F_v = 1.2$, and $G_u = -1$.

In Figure 1(a), $\text{Re}(\lambda_{1,2}(k))$ is plotted for several pairs of self-diffusion coefficients (d_{11}, d_{22}) with fixed $a_{11} = 0.2$ and $a_{22} = 0.3$, and all curves remain strictly negative for every wavenumber $k > 0$. Figure 1(b) shows $\text{Re}(\lambda_{1,2}(k))$ for different self-advection coefficients (a_{11}, a_{22}) with $d_{11} = 0.1$ and $d_{22} = 1$, and again the real parts are negative for all k. Thus, neither varying self-diffusion nor self-advection produces an unstable band of wavenumbers, and no neutral curve arises in this setting. Consistent with Theorem 4.2, the constant equilibrium remains asymptotically stable, so any transport-driven instability in the full RAD system must originate from cross-diffusion or cross-advection. For condition (A) with $G_v = 0$, this result coincides with Theorem 3.4 in [24] and agrees with Corollary 3.8 as a special case of Theorem 3.6, thereby justifying the use of the RAD system without cross terms as a stable reference for the subsequent analysis.

Having established that self-diffusion and self-advection alone do not generate any unstable spatial modes, we now investigate whether the introduction of cross-diffusion can destabilize the constant equilibrium solution. In the case of cross diffusion being present, but cross advection remaining absent; this configuration is further referred to as the RADCD system. With $d_{12}, d_{21} \neq 0$ and $a_{12} = a_{21} = 0$, the system (2.1) reduces to the RADCD system

$$\begin{aligned} \frac{\partial u}{\partial t} &= d_{11}\frac{\partial^2 u}{\partial x^2} + d_{12}\frac{\partial^2 v}{\partial x^2} - a_{11}\frac{\partial u}{\partial x} + F(u,v), \quad x \in \mathbb{R}, t \geq 0, \\ \frac{\partial v}{\partial t} &= d_{21}\frac{\partial^2 u}{\partial x^2} + d_{22}\frac{\partial^2 v}{\partial x^2} - a_{22}\frac{\partial v}{\partial x} + G(u,v), \quad x \in \mathbb{R}, t \geq 0, \\ u(x,0) &= u_0(x), \quad v(x,0) = v_0(x), \quad x \in \mathbb{R}. \end{aligned} \tag{4.5}$$

The corresponding neutral curve provides a natural framework for determining the onset of cross-diffusion–driven instability, as stated in the theorem below.

Theorem 4.3. *Let k^* be the critical neutral point. If $a_{12} = a_{21} = 0$ and condition (A) hold, then the cross-diffusion-driven instability condition for the constant equilibrium solution (u_e, v_e) of RADCD system (4.5) is given by*

$$d_{21} > \bar{d}_{21}(k^*) \text{ when } d_{12} = 0 (\text{ or } d_{12} < \bar{d}_{12}(k^*) \text{ when } d_{21} = 0)$$

for the case $F_v < 0$ and $G_u > 0$,

$$d_{21} < \bar{d}_{21}(k^*) \text{ when } d_{12} = 0 (\text{ or } d_{12} > \bar{d}_{12}(k^*) \text{ when } d_{21} = 0)$$

for the case $F_v > 0$ and $G_u < 0$. The constant equilibrium solution (u_e, v_e) of RADCD system (4.5) is asymptotically stable when

$$d_{21} < \bar{d}_{21}(k^*) \text{ when } d_{12} = 0 (\text{ or } d_{12} > \bar{d}_{12}(k^*) \text{ when } d_{21} = 0)$$

for the case $F_v < 0$ and $G_u > 0$,

$$d_{21} > \bar{d}_{21}(k^*) \text{ when } d_{12} = 0 (\text{ or } d_{12} < \bar{d}_{12}(k^*) \text{ when } d_{21} = 0)$$

for the case $F_v > 0$ and $G_u < 0$.

Proof. By applying an analytical approach similar to that used for RAD system in Theorem 4.2, we derive the condition $\mathrm{Re}(\lambda_{1,2}(k)) = 0$. By simple algebraic manipulation, we obtain

$$\begin{aligned} p_1^2 p_0 =& (- (d_{11} + d_{22})k^2 + (F_u + G_v))^2 (F_u G_v - F_v G_u \\ & - (a_{11}a_{22} - a_{12}a_{21} + d_{11}G_v + d_{22}F_u - d_{12}G_u - d_{21}F_v)k^2 + d_{11}d_{22}k^4) \end{aligned} \tag{4.6}$$

and

$$\begin{aligned} q_0^2 - p_1 q_1 q_0 =& ((a_{11}F_v + a_{22}G_u)k - (a_{11}d_{22} + a_{22}d_{11})k^3)^2 - (- (d_{11} + d_{22})k^2 + (F_u + G_v)) \\ & (a_{11} + a_{22})k((a_{11}F_v + a_{22}G_u)k - (a_{11}d_{22} + a_{22}d_{11})k^3). \end{aligned} \tag{4.7}$$

Next, we substitute (4.6) and (4.7) into (4.1) and simplify the resulting expression to obtain

$$\begin{aligned}(F_u + G_v - (d_{11} + d_{22})k^2)^2(F_uG_v - F_vG_u - (d_{22}F_u + d_{11}G_v - d_{21}F_v - d_{12}G_u)k^2 \\ +(d_{11}d_{22} - d_{12}d_{21})k^4) = k^2(a_{11} - a_{22})^2(F_u - d_{11}k^2)(-G_v + d_{22}k^2).\end{aligned} \tag{4.8}$$

Since we assume that $F_u < 0, G_v < 0, F_uG_v - F_vG_u > 0$, and $d_{11}d_{22} - d_{12}d_{21} > 0$, then $k^2(a_{11} - a_{22})^2(F_u - d_{11}k^2)(-G_v + d_{22}k^2) < 0$ and $(F_u + G_v - (d_{11} + d_{22})k^2)^2 > 0$.

Using simple calculations for (4.8), we obtain the neutral curve

$$d_{21}(k) = \frac{1}{k^2}\Big(G_u + \frac{(F_u - d_{11}k^2)(-G_v + d_{22}k^2)((a_{11} - a_{22})^2k^2 + (F_u + G_v - (d_{11} + d_{22})k^2)^2}{F_v(F_u + G_v - (d_{11} + d_{22})k^2)^2}\Big)$$

when $d_{12} = 0$ and

$$d_{12}(k) = \frac{1}{k^2}\Big(F_v + \frac{(F_u - d_{11}k^2)(-G_v + d_{22}k^2)((a_{11} - a_{22})^2k^2 + (F_u + G_v - (d_{11} + d_{22})k^2)^2}{G_u(F_u + G_v - (d_{11} + d_{22})k^2)^2}\Big)$$

when $d_{21} = 0$. For all wavenumbers k, the trace of the linearized system satisfies $F_u + G_v - (d_{11} + d_{22})k^2 < 0$. Moreover, the asymptotic behavior near the singular point and at large wavenumbers is given by $d_{21}(k) \sim -\frac{\Lambda_J}{F_vk^2}$, $d_{12}(k) \sim -\frac{\Lambda_J}{G_uk^2}$ for $k \to 0$ and $d_{21}(k) \sim -\frac{d_{11}d_{22}}{F_v}k^2$, $d_{12}(k) \sim -\frac{d_{11}d_{22}}{G_u}k^2$ for $k \to \infty$.

For the case $F_v < 0$ and $G_u > 0$, $d_{21}(k) \to \infty$ and $d_{12}(k) \to -\infty$ as $k \to 0$ and $k \to \infty$. Since $d_{21}(k)$ and $d_{12}(k)$ are continuous on $(0, \infty)$, $d_{21}(k)$ attains a global minimum at some $k^* > 0$. Moreover, the two neutral curves are not independent. Since $F_vd_{21}(k) = G_ud_{12}(k)$ for $k > 0$, then $\frac{d_{12}(k)}{d_{21}(k)} = \frac{F_v}{G_u}$. Because $F_v/G_u < 0$, the global minimum of $d_{21}(k)$ corresponds to the global maximum of $d_{12}(k)$ at the same wavenumber $k^* > 0$. We denote these critical values by $\bar{d}_{21}(k^*)$ and $\bar{d}_{12}(k^*)$. If $d_{21} > \bar{d}_{21}(k^*)$ when $d_{12} = 0$ or $d_{12} < \bar{d}_{12}(k^*)$ when $d_{21} = 0$, then the system admits neutral points, and instability may be induced by the cross-diffusion term. If $d_{21} < \bar{d}_{21}(k^*)$ when $d_{12} = 0$ or $d_{12} > \bar{d}_{12}(k^*)$ when $d_{21} = 0$, then no neutral points arise and the cross-diffusion term does not induce instability.

For the case $F_v > 0$ and $G_u < 0$, $d_{21}(k) \to -\infty$ and $d_{12}(k) \to \infty$ as $k \to 0$ and $k \to \infty$. Since $F_v/G_u < 0$ still holds, the identity $\frac{d_{12}(k)}{d_{21}(k)} = \frac{F_v}{G_u}$ again implies that both extrema occur at the same wavenumber $k^* > 0$. In this case, $d_{21}(k)$ attains a global maximum, whereas $d_{12}(k)$ attains a global minimum at k^*. If $d_{21} < \bar{d}_{21}(k^*)$ when $d_{12} = 0$ or $d_{12} > \bar{d}_{12}(k^*)$ when $d_{21} = 0$, then there exist neutral points, and the cross-diffusion term can induce instability. If $d_{21} > \bar{d}_{21}(k^*)$ when $d_{12} = 0$ or $d_{12} < \bar{d}_{12}(k^*)$ when $d_{21} = 0$, then there are no neutral points and the cross-diffusion term does not induce instability. □

Theorem 4.3 identifies the critical cross-diffusion thresholds at which the constant equilibrium solution (u_e, v_e) changes its stability, where the sign of F_vG_u determines the direction of the threshold inequality and the side of the neutral curve associated with instability. We therefore deduce that cross-diffusion serves as the sole destabilizing mechanism in system (4.5), capable of inducing instability in an equilibrium that is otherwise asymptotically stable in the absence of cross-diffusion. This phenomenon is hereafter referred to as cross-diffusion-driven instability. The neutral curves $d_{21}(k)$ and $d_{12}(k)$ are derived by setting (4.1) from the linearized dispersion relation of M_k with $a_{12} = a_{21} = 0$ and define the critical boundaries in cross-diffusion parameter space displayed in Figure 2. The gray-shaded region enclosed between these curves constitutes the cross-diffusion-driven instability region, where spatial perturbations grow exponentially. Notably, this mechanism cannot arise in the absence of cross-diffusion, since the constant equilibrium solution remains asymptotically stable when $d_{12} = d_{21} = 0$. In Figure 2(a), instability requires negative $d_{21}(k)$ and positive $d_{12}(k)$, reflecting a configuration in which the cross-diffusion coefficients bear opposite signs consistent with the condition $F_v G_u < 0$ established in Theorem 4.3. In Figure 2(b), it exhibits a mirror-symmetric instability zone requiring positive $d_{21}(k)$ and negative $d_{12}(k)$ in direct accordance with the reversal of the sign of $F_v G_u$. The critical neutral point k^* identifies the wavenumber at which the minimum cross-diffusion magnitude sufficient to destabilize the equilibrium is attained.

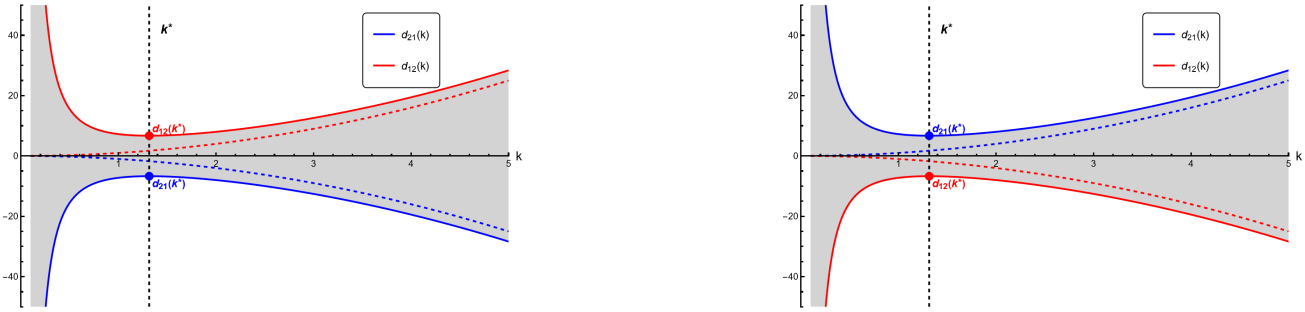

(a) $F_v > 0, G_u < 0$ **(b)** $F_v < 0, G_u > 0$

Figure 2. The neutral curve of $d_{21}(k)$ and $d_{12}(k)$.

With Theorem 4.3 and the simulation in Figure 2, we obtain the following results.

Corollary 4.4. *Assume that $d_{ij} > 0$ for $i, j = 1, 2$ and condition (A), (B), or (C) is satisfied. If $0 < d_{12} < d_{12}(k)$ for the case $F_v > 0$ and $G_u < 0$, $d_{21} = 0$ and $0 < d_{21} < d_{21}(k)$; for the case $F_v < 0$ and $G_u > 0$, $d_{12} = 0$, and then the constant equilibrium solution (u_e, v_e) is unstable where the instability is induced by cross diffusion.*

Accordingly, the following corollary provides a direct consequence of Theorem 3.6. It specifies the algebraic thresholds for d_{12} and d_{21} that mark the transition from the stable homogeneous regime to the cross-diffusion-driven Turing instability region, where spatially heterogeneous structures are expected to develop.

Corollary 4.5. *The condition for cross-diffusion-driven instability of the constant equilibrium solution to the RADCD system (4.5) is given by*

$$F_u + G_v < 0, \quad F_u G_v - F_v G_u > 0, \tag{4.9}$$

$$d_{11} d_{22} - d_{12} d_{21} > 0, \tag{4.10}$$

$$-\frac{1}{4}(a_{11} - a_{22})^2 + d_{22} F_u + d_{11} G_v - d_{21} F_v - d_{12} G_u > 0, \tag{4.11}$$

$$\Big(-\frac{1}{4}(a_{11} - a_{22})^2 + d_{22} F_u + d_{11} G_v - d_{21} F_v - d_{12} G_u \Big)^2 - 4(F_u G_v - F_v G_u)(d_{11} d_{22} - d_{12} d_{21}) > 0. \tag{4.12}$$

Under the conditions of the preceding corollary, the onset of cross-diffusion-driven instability can be further interpreted in terms of the geometry of the cross-diffusion parameter space. The following theorem establishes the existence of an unbounded instability region US_1 in the (d_{12}, d_{21})-plane.

Theorem 4.6. *Assume that assumption (4.9)-(4.12),* $F_u < 0$*,* $G_v < 0$*, and* $F_vG_u < 0$ *hold. If* $d_{12}d_{21} \neq 0$*, then for fixed* d_{11}, d_{22}*, there exists an unbounded region* US_1 *in the* (d_{12}, d_{21})*-plane, defined by*

$$US_1 = \{(d_{12}, d_{21}) \in \mathbb{R}^+ \times \mathbb{R}^+ : d_{22}F_u + d_{11}G_v - d_{21}F_v - d_{12}G_u > \frac{1}{4}(a_{11} - a_{22})^2 \\ +2\sqrt{(F_uG_v - F_vG_u)(d_{11}d_{22} - d_{12}d_{21})}\},$$

such that for any point $(d_{12}, d_{21}) \in US_1$*, the constant equilibrium solution* (u_e, v_e) *with respect to (4.5) is unstable.*

Proof. Based on the assumption that $\Lambda_D = d_{11}d_{22} - d_{12}d_{21} > 0$, we have $d_{11}d_{22} > d_{12}d_{21}$. Therefore, (d_{21}, d_{12}) lies in the region between the two hyperbolic components $d_{12}d_{21} = d_{11}d_{22}$. To show cross-diffusion-driven instability, we must have

$$(d_{11}d_{22} - d_{12}d_{21})k^4 - (-\frac{1}{4}(a_{11} - a_{22})^2 + d_{11}F_u + d_{22}G_v - d_{12}G_u - d_{21}F_v)k^2 + (F_uG_v - F_vG_u) < 0$$

for some k. So, we obtain condition (4.11) and (4.12). Set

$$\begin{aligned} H(d_{12}, d_{21}) =& -\frac{1}{4}(a_{11} - a_{22})^2 + d_{22}F_u + d_{11}G_v - d_{21}F_v - d_{12}G_u \\ L(d_{12}, d_{21}) =& \Big(-\frac{1}{4}(a_{11} - a_{22})^2 + d_{22}F_u + d_{11}G_v - d_{21}F_v - d_{12}G_u\Big)^2 \\ & - 4(F_uG_v - F_vG_u)(d_{11}d_{22} - d_{12}d_{21}). \end{aligned} \tag{4.13}$$

and $\eta = -\frac{1}{4}(a_{11} - a_{22})^2 + d_{11}G_v + d_{22}F_u$.

We show that $H(d_{21}, d_{12}) = 0$ defines a line in the (d_{21}, d_{12})-plane and this line is tangent to the hyperbola $d_{11}d_{22} = d_{12}d_{21}$. Moreover, the line $H(d_{21}, d_{12}) = 0$, the hyperbola $L(d_{21}, d_{12}) = 0$ and the hyperbola $d_{12}d_{21} = d_{11}d_{22}$ intersect at exactly the one common point in the (d_{21}, d_{12})-plane. Let $\theta = d_{21}F_v + d_{12}G_u$ and $\xi = d_{21}F_v - d_{12}G_u$. Then, we have

$$d_{12} = \frac{\theta - \xi}{2G_u}, \quad d_{21} = \frac{\theta + \xi}{2F_v}. \tag{4.14}$$

By substituting (4.14) to (4.13), we get

$$\Big(1 + \frac{\Lambda_J}{F_vG_u}\Big)\theta^2 + 2\eta\theta - \frac{\Lambda_J}{F_vG_u}\xi^2 - 4d_{11}d_{22}\Lambda_J + \eta^2 = 0. \tag{4.15}$$

Furthermore, we have $\Lambda_J = F_uG_v - F_vG_u > 0$, $F_u < 0$, $G_v < 0$, and $F_vG_u < 0$. Then, $\frac{\Lambda_J}{F_vG_u} < 0$, $1 + \frac{\Lambda_J}{F_vG_u} = \frac{F_uG_v}{F_vG_u} < 0$. Equation (4.15) can be rewritten as

$$\frac{F_uG_v}{F_vG_u}\Big(\theta - \frac{F_vG_u}{F_uG_v}\eta\Big)^2 + \frac{-\Lambda_J}{F_vG_u}\xi^2 = -\eta^2\frac{\Lambda_J}{F_vG_u} + 4d_{11}d_{22}\Lambda_J. \tag{4.16}$$

Observe that the right-hand side of (4.16) is positive, so the equation $L(d_{21}, d_{12}) = 0$ defines a hyperbola in the (d_{21}, d_{12})-plane. Furthermore, if (d_{21}, d_{12}) is on the hyperbola $d_{12}d_{21} = d_{11}d_{22}$, $L(d_{21}, d_{12}) = 0$ if and only if $\eta - d_{21}F_v - d_{12}G_u = 0$. So, the hyperbola $d_{12}d_{21} = d_{11}d_{22}$, the hyperbola $L(d_{21}, d_{12}) = 0$, and the line $\eta - d_{21}F_v - d_{12}G_u = 0$ intersect at one point in the (d_{21}, d_{12})-plane.

Therefore, we derive the inequality

$$d_{22}F_u + d_{11}G_v - d_{21}F_v - d_{12}G_u > \frac{1}{4}(a_{11} - a_{22})^2 + 2\sqrt{(F_uG_v - F_vG_u)(d_{11}d_{22} - d_{12}d_{21})}.$$

by taking the positive square root of the condition $L(d_{21}, d_{12}) > 0$. This result follows from the positivity of $H(d_{21}, d_{12}) > 0$ and the fact that (d_{21}, d_{12}) lies outside the hyperbola, as confirmed through direct calculation. □

Theorem 4.6 shows that cross-diffusion-driven instability occurs in an unbounded region of the (d_{21}, d_{12})-plane. Hence, the constant equilibrium solution becomes unstable whenever (d_{21}, d_{12}) lies in US_1. As an illustration, the parameter space US_1 for cross-diffusion-driven instability of RAD system is given in Figure 3. The boundary of the orange region US_1 is primarily by the black hyperbola $d_{12}d_{21} = d_{11}d_{22}$ and by the blue and red critical curves corresponding to $H(d_{21}, d_{12}) = 0$ and $L(d_{21}, d_{12}) = 0$, respectively, evaluated at the critical wavenumber k. The comparison between Figure 3a and 3b reveals that the magnitude and sign of the cross-reaction interactions F_v and G_u significantly affect the shape and area of the instability region, even though both still satisfy the condition $F_vG_u < 0$.

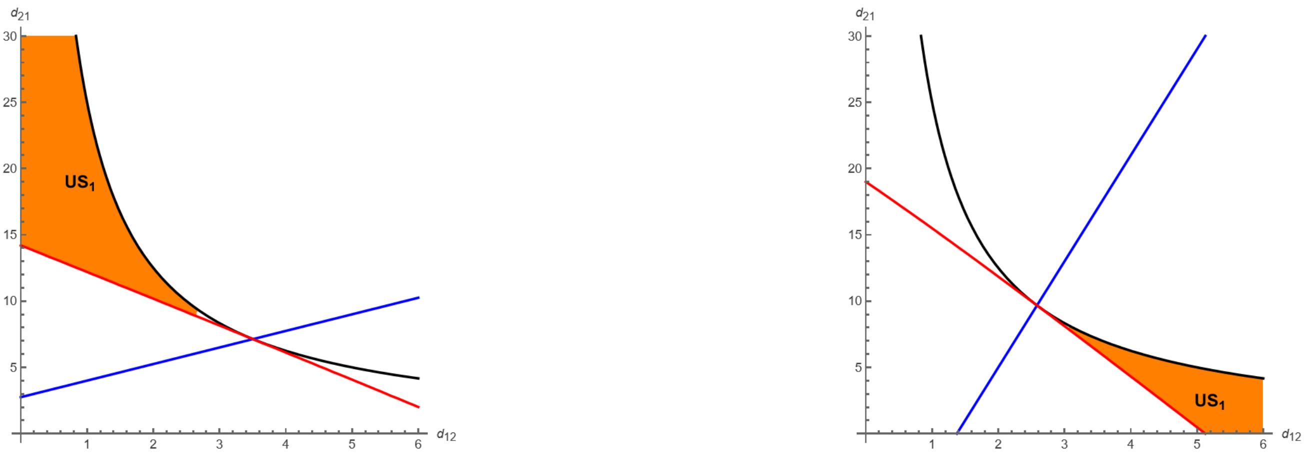

(a) $F_v = -4, G_u = 5$ **(b)** $F_v = 1, G_u = -8$

Figure 3. Parameter space US_1 for cross-diffusion-driven instability of RADCD system. The paramater values are $a_{11} = 3$, $a_{22} = 1$, $d_{11} = 5$, $d_{22} = 5$, $F_u = -1$, $G_v = -1$, and $F_vG_u < 0$.

In Theorem 4.2, we know that self-diffusion and self-advection do not induce instability in the RAD system (4.2). Meanwhile, we know that cross-diffusion can induce instability for system (4.5) in Theorem 4.3. Now, we consider the RAD system with cross-advection, hereafter referred to as the RADCA system

$$\begin{aligned}
\frac{\partial u}{\partial t} &= d_{11}\frac{\partial^2 u}{\partial x^2} - a_{11}\frac{\partial u}{\partial x} - a_{12}\frac{\partial v}{\partial x} + F(u, v), \quad x \in \mathbb{R}, t \geq 0,\\
\frac{\partial v}{\partial t} &= d_{22}\frac{\partial^2 v}{\partial x^2} - a_{21}\frac{\partial u}{\partial x} - a_{22}\frac{\partial v}{\partial x} + G(u, v), \quad x \in \mathbb{R}, t \geq 0,\\
u(x, 0) &= u_0(x), \quad v(x, 0) = v_0(x), \quad x \in \mathbb{R},
\end{aligned} \tag{4.17}$$

for $d_{12} = d_{21} = 0$. Next, we analyze the linear stability analysis for the RADCA system for $d_{11} \neq d_{22}$ and $a_{11} \neq a_{22}$ and we obtain the following results.

Corollary 4.7 (RADCA system)**.** *If $d_{12} = d_{21} = 0$ and condition (A) hold, then the constant equilibrium solution (u_e, v_e) of system (4.17) is asymtotically stable.*

Proof. By Theorem 3.6, we have

$$\Lambda_A - \frac{1}{4}\tau_A^2 + \tau_{DJ} = -a_{12}a_{21} - \frac{1}{4}(a_{11} - a_{22})^2 + d_{11}F_u + d_{22}G_v < 0.$$

This inequality follows directly from the assumptions $F_u < 0$, $G_v < 0$, $F_u + G_v < 0$, and $F_uG_v - F_vG_u > 0$. Consequently, the constant equilibrium solution (u_e, v_e) of system (4.17) remains asymptotically stable. □

Theorem 4.8. *Let k^* be the critical neutral point. Assume condition (B) or (C), $F_u + G_v < 0$, and $F_uG_v - F_vG_u > 0$ hold, $d_{11} \neq d_{22}$, and $a_{11} \neq a_{22}$. The condition for cross-advection-driven instability of the constant equilibrium solution (u_e, v_e) of RADCA system (4.17) is given by*

$$a_{12}^2 > \bar{a}_{12}^2(k^*) \text{ when } a_{21} = 0 \text{ or } a_{21}^2 > \bar{a}_{21}^2(k^*) \text{ when } a_{12} = 0.$$

The constant equilibrium solution (u_e, v_e) is locally stable when

$$a_{12}^2 < \bar{a}_{12}^2(k^*) \text{ when } a_{21} = 0 \text{ or } a_{21}^2 < \bar{a}_{21}^2(k^*) \text{ when } a_{12} = 0.$$

Proof. By substituting $d_{12} = d_{21} = 0$ into (4.1), we obtain the neutral curve

$$\begin{aligned} a_{12}^2(k) =& \frac{1}{4G_u^2k^2}\Big((a_{22} - a_{11})(F_u - G_v - (d_{11} - d_{22})k^2)k + (F_u + G_v - (d_{11} + d_{22})k^2) \\ & \sqrt{(-4F_vG_u + 4F_uG_v + (a_{11} - a_{22})k^2 - 4d_{22}F_uk^2 - 4d_{11}G_vk^2 + 4d_{11}d_{22}k^4}\Big)^2 \end{aligned}$$

when $a_{21} = 0$, and

$$\begin{aligned} a_{21}^2(k) =& \frac{1}{4F_v^2k^2}\Big((a_{22} - a_{11})(F_u - G_v - (d_{11} - d_{22})k^2)k + (F_u + G_v - (d_{11} + d_{22})k^2) \\ & \sqrt{(-4F_vG_u + 4F_uG_v + (a_{11} - a_{22})k^2 - 4d_{22}F_uk^2 - 4d_{11}G_vk^2 + 4d_{11}d_{22}k^4}\Big)^2 \end{aligned}$$

when $a_{12} = 0$. Set

$$\begin{aligned} S_2(k) =& \frac{1}{4k^2}\Big((a_{22} - a_{11})(F_u - G_v - (d_{11} - d_{22})k^2)k + (F_u + G_v - (d_{11} + d_{22})k^2) \\ & \sqrt{(-4F_vG_u + 4F_uG_v + (a_{11} - a_{22})k^2 - 4d_{22}F_uk^2 - 4d_{11}G_vk^2 + 4d_{11}d_{22}k^4}\Big)^2 \end{aligned}$$

Since the conditions (A), (B), or (C), $F_u + G_v < 0$, and $F_uG_v - F_vG_u > 0$ hold, then $S_2(k) > 0$ for all wavenumbers k. A straightforward analysis demonstrates that $S_2(k) \to \infty$ as $k \to 0$ and $k \to \infty$. Therefore, the function $S_2(k)$ attains its minimum at k^*. If the function $S_2(k)$ attains its minimum at k^*, then the corresponding critical neutral point is given by $\bar{a}_{12}^2(k^*)$ (or $\bar{a}_{21}^2(k^*)$ for the neutral curve $a_{12}^2(k)$ (or $a_{21}^2(k)$). When $a_{12}^2 = \bar{a}_{12}^2(k^*)$ (or $a_{21}^2 = \bar{a}_{21}^2(k^*)$), we obtain $Re(\lambda_{1,2}(k^*)) = 0$, thereby identifying the critical threshold for cross-advection-induced instability of the constant equilibrium solutions. If $a_{12}^2 > \bar{a}_{12}^2(k^*)$ (or $a_{21}^2 > \bar{a}_{21}^2(k^*)$), then neutral points occur and the cross-advection term can induce instability. If $a_{12}^2 < \bar{a}_{12}^2(k^*)$ (or $a_{21}^2 < \bar{a}_{21}^2(k^*)$), then no neutral point arises and the cross-advection term does not induce instability. □

Theorem 4.8 generalizes the cross-advection-driven instability result of [24] (see Theorem 3.5), which was obtained under $d_{11} = d_{22}$, $a_{11} = a_{22}$, and condition (B) with $G_v = 0$. Theorem 4.8 removes all three constraints simultaneously and establishes the instability criterion in the fully general setting $d_{11} \neq d_{22}$, $a_{11} \neq a_{22}$, and $G_v \neq 0$. Figure 4 gives a geometric representation of this generalization through the neutral curves $a_{12}^2(k)$ and $a_{21}^2(k)$. The left panel corresponds to the case $a_{21} = 0$, while the right panel corresponds to the case $a_{12} = 0$. Each curve exhibits a clear minimum at its critical neutral point, namely $(k_{12}^*, a_{12}^2(k_{12}^*))$ and $(k_{21}^*, a_{21}^2(k_{21}^*))$, respectively. Moreover, both minima occur at the same critical wavenumber, so that $k_{12}^* = k_{21}^*$. This common critical wavenumber indicates that the onset of instability in the two one-sided cross-advection configurations is associated with the same dominant spatial scale. Hence, the region below each neutral curve represents the cross-advection-driven instability zone, where the constant equilibrium solution (u_e, v_e) loses stability and spatially heterogeneous patterns may emerge.

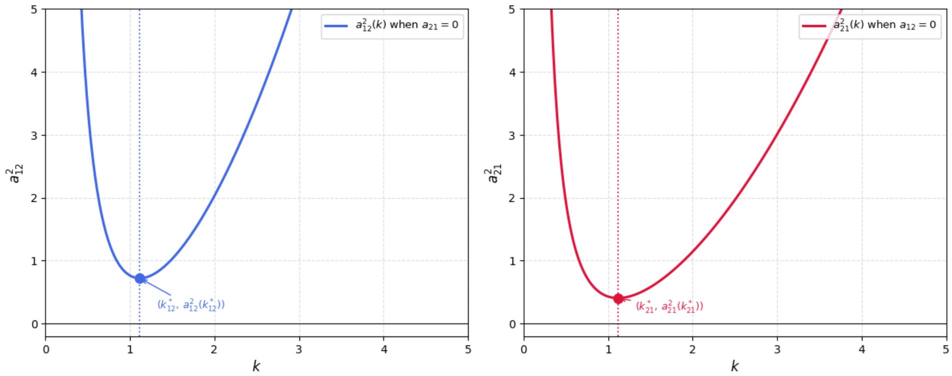

Figure 4. Neutral curves for cross-advection-driven instability.

Having established the dispersion-theoretic evidence for cross-advection-driven instability, we now characterize the parameter space (a_{12}, a_{21}) within which such instability occurs. Building on the linear stability analysis in Theorem 3.6, the following corollary identifies the explicit algebraic conditions on(a_{12}, a_{21}) under which the constant equilibrium solution (u_e, v_e) loses stability, delineating the precise region in the (a_{12}, a_{21})-plane where spatially heterogeneous patterns emerge.

Corollary 4.9. *The condition for cross-diffusion-driven instability of the constant equilibrium solution to the RADCD system (4.17) is given by*

$$F_u + G_v < 0, \quad F_u G_v - F_v G_u > 0, \tag{4.18}$$

$$a_{11}a_{22} - a_{12}a_{21} > 0, \tag{4.19}$$

$$a_{11}a_{22} - a_{12}a_{21} - \frac{1}{4}(a_{11} + a_{22})^2 + d_{22}F_u + d_{11}G_v > 0, \tag{4.20}$$

$$\left(a_{11}a_{22} - a_{12}a_{21} - \frac{1}{4}(a_{11} + a_{22})^2 + d_{22}F_u + d_{11}G_v\right)^2 - 4(F_u G_v - F_v G_u)(d_{11}d_{22} - d_{12}d_{21}) > 0. \tag{4.21}$$

The onset of cross-advection-driven instability can be interpreted geometrically through the cross-advection parameter space. The following theorem establishes the existence of an unbounded instability region US_2 in the (a_{12}, a_{21})-plane.

Theorem 4.10. *Consider*

$$H_1(a_{12}, a_{21}) = a_{11}a_{22} - a_{12}a_{21} - \frac{1}{4}(a_{11} + a_{22})^2 + d_{22}F_u + d_{11}G_v,$$

and

$$L_1(a_{12}, a_{21}) = (a_{11}a_{22} - a_{12}a_{21} - \frac{1}{4}(a_{11} + a_{22})^2 + d_{22}F_u + d_{11}G_v)^2 - 4(F_uG_v - F_vG_u)(d_{11}d_{22}).$$

If $a_{12}a_{21} \neq a_{11}a_{22}$, then for fixed $d_{11}, d_{22}, a_{11}, a_{22}$, there exists an unbounded region US_2 in the (a_{12}, a_{21})-plane, defined by

$$US_2 = \{(a_{12}, a_{21}) \in \mathbb{R}^+ \times \mathbb{R}^+ : a_{11}a_{22} - a_{12}a_{21} > 0, H_1(a_{12}, a_{21}) > 0, L_1(a_{12}, a_{21}) > 0\}$$

such that for any point $(a_{12}, a_{21}) \in US_2$, the constant equilibrium solution (u_e, v_e) with respect to (4.17) is unstable.

Proof. According to the assumption that $a_{11}a_{22}-a_{12}a_{21} > 0$, we have $a_{12}a_{21} < a_{11}a_{22}$. The area below of the hyperbola $a_{12}a_{21} = a_{11}a_{22}$ is also located in quadrant I. Next, $H_1(a_{12}, a_{21}) > 0$ is also an area under the hyperbola $a_{12}a_{21} = d_{11}G_v + d_{22}F_u - \frac{1}{4}(a_{11} - a_{21})^2$. Since $-a_{12}a_{21} - \frac{1}{4}(a_{11} - a_{21})^2 + d_{11}G_v + d_{22}F_u > 0$, condition $L_1(a_{12}, a_{21})$ can be simplified to

$$a_{12}a_{21} < -\frac{1}{4}(a_{11} - a_{22})^2 + d_{11}G_v + d_{22}F_u - 2\sqrt{(F_uG_v - F_vG_u)d_{11}d_{22}}.$$

So, US_2 is the set of positive points (a_{12}, a_{21}) that lie below the three hyperbolas. In other words, $US_2 \neq \emptyset$ if and only if $a_{12}a_{21} < \min\{a_{11}a_{22}, -\frac{1}{4}(a_{11} - a_{22})^2 + d_{11}G_v + d_{22}F_u, -\frac{1}{4}(a_{11} - a_{22})^2 + d_{11}G_v + d_{22}F_u - 2\sqrt{(F_uG_v - F_vG_u)d_{11}d_{22}}\}$ □

Theorem 4.10 shows that cross-advection-driven instability occurs in an unbounded region of the (a_{12}, a_{21})-plane. Hence, the constant equilibrium solution becomes unstable whenever (a_{12}, a_{21}) lies in US_2 (see Figure 5).

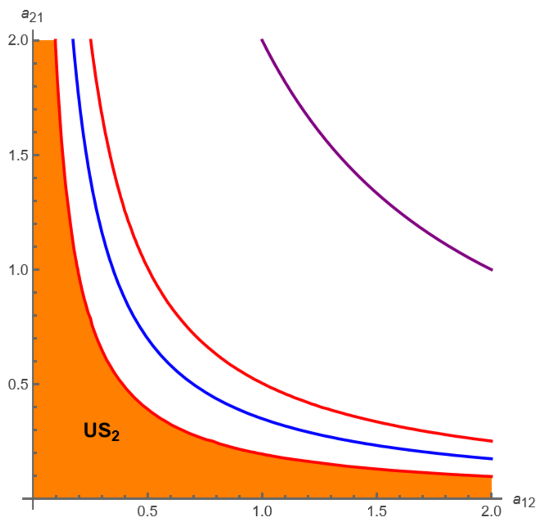

Figure 5. Parameter space US_2 of RADCA system with $a_{11} = 1$, $a_{22} = 2$, $d_{11} = 2$, $d_{22} = 3$, $F_u = 1$, $G_v = -1.2$, $F_v = 1$, and $G_u = -1.201$.

The shaded domain represents parameter combinations satisfying all analytical conditions for instability under the combined effects of reaction kinetics, diffusion, and cross-advection. The purple curve denotes $a_{11}a_{22} - a_{12}a_{21} = 0$, the blue curve denotes $H_1(a_{12}, a_{21})$, and the red dashed curve denotes $L_1(a_{12}, a_{21})$. These boundaries characterize the transition between stability regions and spectral regimes in the parameter space. Their intersections determine an unbounded region in parameter space. Within this region, the constant equilibrium solution remains stable in the absence of spatial transport, but asymmetric cross-advection effects destabilize it and thereby induce pattern formation.

Based on Theorem 4.2, self-diffusion and self-advection do not induce instability of the constant equilibrium solution under the prescribed stability assumptions. In contrast, Theorems 4.3-4.8 demonstrate that cross-diffusion and cross-advection may independently destabilize the system when they are incorporated into the RAD framework. Motivated by these results, it remains necessary to examine whether the joint presence of cross-diffusion and cross-advection can destabilize the equilibrium when the RAD model is generalized to the full RADCDCA framework. To address this issue, we reconsider the RADCDCA system (2.1).

Theorem 3.6 provides a complete characterization of the linear stability region in which the constant equilibrium solution (u_e, v_e) remains stable whenever it satisfies $\tau_J < 0$, $\Lambda_J > 0$ and one of the two conditions stated in (3.21) or (3.22)-(3.23). Consequently, if the conditions $\tau_J < 0$, $\Lambda_J > 0$ continue to hold while conditions (3.22) and (3.23) become positive, then the stability criteria established in Theorem 3.6 are no longer satisfied. From a spectral viewpoint, this situation implies that the characteristic polynomial (3.12) admits a positive real root for some wavenumber k. In other words, the constant equilibrium solution loses its linear stability. The following theorem states the instability conditions induced by cross-diffusion and cross-advection, which constitute the logical complement of Theorem 3.6.

Theorem 4.11. *The conditions for cross-diffusion- and cross-advection-driven instability in the RADCDCA system are given by*

$$\Lambda_A > 0, \quad \Lambda_D > 0, \tag{4.22}$$

$$\tau_J < 0, \quad \Lambda_J > 0, \tag{4.23}$$

$$\Lambda_A - \frac{1}{4}\tau_A^2 + \tau_{DJ} > 0, \tag{4.24}$$

$$(\Lambda_A - \frac{1}{4}\tau_A^2 + \tau_{DJ})^2 - 4\Lambda_D\Lambda_J > 0. \tag{4.25}$$

Theorem 4.11 identifies the fundamental conditions under which the RADCDCA system undergoes cross-diffusion- and cross-advection-driven instability. Under conditions (4.22)-(4.25), the polynomial (3.19) has two distinct positive roots

$$k_\pm^2 = \frac{\Lambda_A - \frac{1}{4}\tau_A^2 + \tau_{DJ} \pm \sqrt{(\Lambda_A - \frac{1}{4}\tau_A^2 + \tau_{DJ})^2 - 4\Lambda_D\Lambda_J}}{2\Lambda_D},$$

for $0 < k^- < k_+^2$. Consequently, the polynomial (3.19) is negative for $k_-^2 < k^2 < k_+^2$, implying that two eigenvalues have opposite signs. Therefore, one eigenvalue is positive for every k in this interval, and the constant equilibrium solution is unstable to spatial pertubations. In particular, it shows that the constant equilibrium solution may lose stability even when the underlying ODE equilibrium remains stable, provided that the transport-induced quantities Λ_A, Λ_D, τ_J, Λ_J, $\Lambda_A - \frac{1}{4}\tau_A^2 + \tau_{DJ}$, and $(\Lambda_A - \frac{1}{4}\tau_A^2 + \tau_{DJ})^2 - 4\Lambda_D\Lambda_J$ satisfy the stated sign conditions. Therefore, the theorem gives an explicit analytical criterion for detecting instability generated by the combined action of cross-diffusion and cross-advection.The following is a direct consequence of Theorem 4.11.

Corollary 4.12 (Self-diffusion-driven instability of RD system)**.** *Assume that $d_{12} = d_{21} = 0$, $a_{11} = a_{22} = a_{21} = a_{12} = 0$, and one of the conditions (A), (B), or (C) holds. The conditions for self-diffusion-driven instability at the constant equilibrium solution (u_e, v_e) of RD system are given by*

$$\begin{aligned} F_u + G_v < 0, \quad F_uGv - F_vG_u &<0, \\ d_{11}G_v + d_{22}F_u &>0, \\ (d_{11}G_v + d_{22}F_u)^2 - 4d_{11}d_{22}(F_uG_v - F_vG_u) &>0. \end{aligned}$$

The condition for instability driven by self-diffusion in Corollary 4.12 that we obtained is the same as that obtained by [24] (see Theorem 2.1) for condition (A), [32] (see Theorem 2.2) for condition (B), [22], and [3] (see page 367) for condition (C).

Corollary 4.13 (Cross-diffusion-driven instability of RD system)**.** *Assume that $a_{11} = a_{22} = a_{21} = a_{12} = 0$, and one of the conditions (A), (B), or (C) holds. The constant equilibrium solution (u_e, v_e) of RD system is cross-diffusion-driven instability if*

$$\begin{aligned} F_u + G_v < 0, \quad F_uGv - F_vG_u &<0, \\ d_{11}d_{22} - d_{12}d_{21} &>0, \\ d_{11}G_v + d_{22}F_u - d_{12}G_u - d_{21}F_v &>0, \\ (d_{11}G_v + d_{22}F_u - d_{12}G_u - d_{21}F_v)^2 - 4(d_{11}d_{22} - d_{12}d_{21})(F_uG_v - F_vG_u) &>0. \end{aligned}$$

The conditions for cross-diffusion driven instability in Corollary 4.13 are also the same as that investigated by [24] (see Theorem 2.3), [32] (see Theorem 2.1), [23] (see Theorem 1), and [37] (see Theorem 7). Corollary 4.12 and 4.13 are conditions of instability induced by self-diffusion and cross-diffusion for the RD systems.

The unbounded region US_3 in the (a_{12}, d_{12})-plane where cross-advection- and cross-diffusion-induced instability is given in the following lemma.

Theorem 4.14. *Consider*

$$H_2(a_{12}, d_{12}) = -a_{12}^2 - \frac{1}{4}(a_{11} - a_{22})^2 + d_{22}F_u + d_{11}G_v - d_{12}(F_v + G_u)$$

and

$$L_2(a_{12}, d_{12}) = (H_2(a_{12}, d_{12}))^2 - 4(F_uG_v - F_vG_u)(d_{11}d_{22} - d_{12}^2).$$

If $a_{12}a_{21} \neq a_{11}a_{22}$, $d_{12}d_{21} \neq d_{11}d_{22}$, $d_{12} = d_{21}$, and $a_{12} = a_{21}$, then for fixed d_{11}, d_{22}, a_{11}, and a_{22}, there exists an unbounded region US_3 in the (a_{12}, d_{12})-plane, defined by

$$\begin{aligned} US_3 =&\{(a_{12}, d_{12} \in \mathbb{R}^+ \times \mathbb{R}^+) : a_{11}a_{22} - a_{12}^2 > 0, d_{11}d_{22} - d_{12}^2 > 0, \\ &H_2(a_{12}, d_{12}) > 0, L_2(a_{12}, d_{12}) > 0\} \end{aligned}$$

such that for any point $(a_{12}, d_{12}) \in US_3$, the constant equilibrium solution (u_e, v_e) with respect to (4.17) is unstable.

Proof. We start from the assumption that $d_{11}d_{22} - d_{12}^2 > 0$ and $a_{11}a_{22} - a_{12}^2 > 0$. Since $d_{12} = d_{21}$ and $a_{12} = a_{21}$, we obtain $d_{12}^2 < d_{11}d_{22}$ and $a_{12}^2 < a_{11}a_{22}$. The inequality $d_{12}^2 < d_{11}d_{22}$ is the region below the line $d_{12}^2 = d_{11}d_{22}$ and above the line $d_{12} = 0$. Meanwhile, the inequality $a_{12}^2 < a_{11}a_{22}$ is the region to the left of the line $a_{12}^2 = a_{11}a_{22}$ and to the right of the line $a_{12} = 0$. Thus, we obtain the intersection of the regions satisfying the inequalities $d_{12}^2 < d_{11}d_{22}$ and $a_{12}^2 < a_{11}a_{22}$ in the form of a rectangle.

Now, we consider the region satisfying the inequalities $H_2(a_{12}, d_{12}) > 0$ and $L_2(a_{12}, d_{12}) > 0$. Since $F_v + G_u < 0$, then $H_2(a_{12}, d_{12}) = 0$ is an upward-facing parabola with its vertex located at $\left(0, \frac{d_{22}F_u + d_{11}G_v - \frac{1}{4}(a_{11}-a_{22})^2}{F_v + G_u}\right)$. Since $H_2(a_{12}, d_{12}) > 0$, then inequality $L_2(a_{12}, d_{12}) > 0$ focuses on the branch $H_2(a_{12}, d_{12}) = 2\sqrt{(F_uG_v - F_vG_u)(d_{11}d_{22} - d_{12}^2)}$. This shows that the boundary of a_{12}^2 is a function of d_{12} or vice versa, as written below:

$$a_{12}^2 = -\frac{1}{4}(a_{11} - a_{22})^2 + d_{22}F_u + d_{11}G_v - d_{12}(F_v + G_u) - 2\sqrt{(F_uG_v - F_vG_u)(d_{11}d_{22} - d_{12}^2)}.$$

The graph will be a descending parabola or inverted parabola, but curved by the root term that depends on d_{12}. Since $d_{11}d_{22} - d_{12}^2 \to 0$ as $d_{12} \to \sqrt{d_{11}d_{22}}$ and $F_uG_v - F_vG_u > 0$, it follows that $\sqrt{(F_uG_v - F_vG_u)(d_{11}d_{22} - d_{12}^2)} \to 0$. Because $H_2(a_{12}, d_{12})$ decreases with respect to a_{12}^2, the term $H_2(a_{12}, d_{12}) > 2\sqrt{(F_uG_v - F_vG_u)(d_{11}d_{22} - d_{12}^2)}$ describes the region above the root curve $(F_uG_v - F_vG_u)(d_{11}d_{22} - d_{12}^2)$ but below the downward-opening parabola. Furthermore, the rectangular region bounded by the strip $d_{11}d_{22} > d_{12}^2$ and $a_{11}a_{22} > a_{12}^2$ intersects with the parabola $H_2(a_{12}, d_{12}) > 0$ and the curve $L_2(a_{12}, d_{12}) > 0$ at one point in the plane $(a_{12}, d_{12}) \in \mathbb{R}^+ \times \mathbb{R}^+$. □

An illustration of the unstable region US_3 is shown in Figure 6. The purple, black, blue, and red curves represent the zero-level boundaries $a_{11}a_{22} - a_{12}^2 = 0$, $d_{11}d_{22} - d_{12}^2 = 0$, $H_2(a_{12}, d_{12}) = 0$, and $L_2(a_{12}, d_{12}) = 0$, respectively. These boundaries divide the (a_{12}, d_{12})-plane into spectrally stable and unstable subregions.

The stability region consists of parameter values for which all Routh-Hurwitz conditions in Theorem 3.6 are strictly satisfied, so that the real parts of all eigenvalues of system (3.12) remain negative for every positive wavenumber k. In contrast, the shaded region US_3 represents the instability domain generated by cross-diffusion and cross-advection. In this region, the constant equilibrium is stable in the absence of cross-transport effects, but the inclusion of cross-diffusion and cross-advection violates at least one stability condition and produces eigenvalues with positive real parts. It is worth noting that, once cross-diffusion ($d_{12} = d_{21}$) destabilizes the system, symmetric cross-advection ($a_{12} = a_{21}$) does not restore stability. Instead, it may amplify the instability and reshape the resulting spatiotemporal patterns by modifying their direction, intensity, and propagation behavior. Based on Theorem 3.6–4.14, we obtain the following remark.

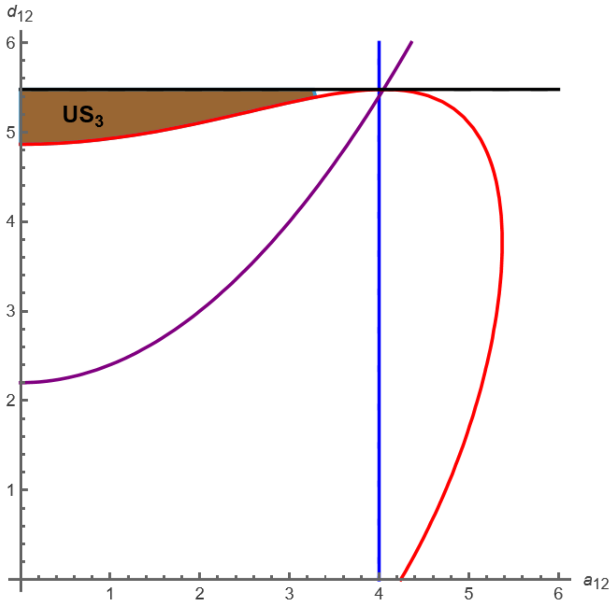

Figure 6. Parameter space US_3 of RADCDCA system with $a_{11} = 4$, $a_{22} = 4$, $d_{11} = 5$, $d_{22} = 6$, $F_u = -1$, $G_v = -1$, $F_v = 1$, $G_u = -6$, $d_{12} = d_{21}$, and $a_{12} = a_{21}$.

Remark 4.15. *Assume that condition (A) holds, namely $F_u < 0$, $G_v < 0$, $F_vG_u < 0$, $F_u + G_v < 0$, and $F_uG_v - F_vG_u > 0$. Then, the constant equilibrium (u_e, v_e) is asymptotically stable for the corresponding ODE system. Moreover, this stability is preserved in the RAD system (4.2) and also in the RADCA system (4.17). Cross-diffusion may destabilize the constant equilibrium when it acts alone in the RADCD system (4.5) or interacts with cross-advection in the full RADCDCA system (2.1). The resulting loss of stability can therefore be interpreted as a cross-transport-induced instability, not as an instability inherited from the local reaction dynamics.*

Under conditions (B) and (C), the situation changes substantially when asymmetric cross-advection occurs in the RADCA system with $a_{12} \neq a_{21}$ and $d_{12} = d_{21} = 0$. In this case, the off-diagonal advection terms no longer act symmetrically in the characteristic polynomial (3.12). As a result, the imaginary contribution to the dispersion matrix may alter the spectral structure and generate instability bands that do not appear in the symmetric cross-advection setting. Therefore, the sign and degree of asymmetry of the cross-advection coefficients play an important role in determining the qualitative dynamics, including the location and width of unstable wavenumber bands and the possible emergence of wave-type instability mechanisms. This observation provides the motivation for applying the preceding theoretical results to a concrete ecological model. In the next section, we consider a predator–prey system to examine how these stability mechanisms appear in terms of coexistence, species movement, and pattern formation.

5. Application to predator-prey model

In mathematical ecology, the RAD system provides a more realistic framework for describing spatial predator-prey dynamics than the classical Lotka-Volterra model. This is because population movement depends not only on local interactions, but also on diffusion and directed transport. To illustrate the theoretical results established above, we consider the RADCDCA system

$$\begin{aligned}
&\frac{\partial u}{\partial t} = d_{11}\frac{\partial^2 u}{\partial x^2} + d_{12}\frac{\partial^2 v}{\partial x^2} - a_{11}\frac{\partial u}{\partial x} - a_{12}\frac{\partial v}{\partial x} + u(\alpha_1 - \beta_1 u + c_1 v), \quad x \in \mathbb{R}, t \geq 0\\
&\frac{\partial v}{\partial t} = d_{21}\frac{\partial^2 u}{\partial x^2} + d_{22}\frac{\partial^2 v}{\partial x^2} - a_{21}\frac{\partial u}{\partial x} - a_{22}\frac{\partial v}{\partial x} + v(\alpha_2 - \beta_2 u - c_2 v), \quad x \in \mathbb{R}, t \geq 0\\
&u(x,0) = u_0(x), \quad v(x,0) = v_0(x), \quad x \in \mathbb{R}.
\end{aligned} \tag{5.1}$$

Here, $u(x,t)$ and $v(x,t)$ denote the spatial densities of prey and predator, respectively. Ecologically, d_{11} and d_{22} reflect the natural spatial spreading of prey and predator, while d_{12} and d_{21} capture how each species adjusts its distribution in response to the other species. Meanwhile, a_{12} represents directed prey movement caused by predator presence, such as avoidance behavior, and a_{21} represents directed predator movement toward prey-rich regions.

The local population dynamics are governed by

$$F(u,v) = u(\alpha_1 - \beta_1 u + c_1 v) \text{ and } G(u,v) = v(\alpha_2 - \beta_2 u - c_2 v), \tag{5.2}$$

where all parameters $\alpha_1, \alpha_2, \beta_1, \beta_2, c_1, c_2$ are positive. The parameters α_1 and α_2 describe the intrinsic growth rates of prey and predator, while β_1 and c_2 measure density-dependent competition. The coefficient c_1 captures the positive feedback of predators on prey growth, whereas β_2 represents the negative effect of prey on predator growth. Thus, this non-classical predator–prey model is useful for analyzing how transport interactions affect the stability of the constant equilibrium solution and generate pattern formation.

Before we analyze spatial dynamics such as linear stability and pattern formation, the fundamental step is to identify constant equilibrium solutions that are independent of both space and time. Thus, system (5.1) has four non-negative constant equilibrium solutions

$$E_0 = (0,0), \quad E_1 = \Big(0, \frac{\alpha_2}{c_2}\Big), \quad E_2 = \Big(\frac{\alpha_1}{\beta_1}, 0\Big), \quad E_3 = \Big(\frac{\alpha_1 c_2 + \alpha_2 c_1}{\beta_1 c_2 + \beta_2 c_1}, \frac{\alpha_2\beta_1 - \alpha_1\beta_2}{\beta_1 c_2 + \beta_2 c_1}\Big). \tag{5.3}$$

Based on the assumption that $\alpha_1, \alpha_2, \beta_1, \beta_2, c_1, c_2 > 0$, we obtain $\frac{\alpha_2}{c_2} > 0$, $\frac{\alpha_1}{\beta_1} > 0$, and the coexistence equilibrium E_3 is positive if and only if $\alpha_2\beta_1 - \alpha_1\beta_2 > 0$. The constant equilibrium solutions in (5.3) are also the equilibrium points of the ODE system

$$\begin{aligned}
\frac{du}{dt} &= u(\alpha_1 - \beta_1 u + c_1 v),\\
\frac{dv}{dt} &= v(\alpha_2 - \beta_2 u - c_2 v).
\end{aligned} \tag{5.4}$$

Next, we analyze the stability of the equilibrium points in (5.3) for system (5.4) to understand how the system responds to small disturbances around that equilibrium point.

Lemma 5.1. *Suppose that all parameters of system* (5.4) *are positive. If* $\frac{\alpha_2}{\alpha_1} > \frac{\beta_2}{\beta_1}$, *then* E_0 *is an unstable node,* E_1 *and* E_2 *are saddle points, and the positive coexistence equilibrium* E_3 *is asymptotically stable.*

Proof. The Jacobian matrix of system (5.4) at the constant equilibrium solution (u_e, v_e) is given by

$$J = \begin{pmatrix} \alpha_1 - 2\beta_1 u_e + c_1 v_e & c_1 u_e \\ -\beta_2 v_e & \alpha_2 - \beta_2 u_e - 2c_2 v_e \end{pmatrix}.$$

We have sufficiently proven that condition (2.3) is satisfied for every equilibrium solution. First, we obtain that evaluating the trace and determinant condition (2.3) at the trivial equilibrium E_0 yields

$$\mathrm{Tr}(J)\Big|_{E_0} = \alpha_1 + \alpha_2 > 0, \qquad \det(J)\Big|_{E_0} = \alpha_1\alpha_2 > 0.$$

Thus, both eigenvalues have positive real parts. Consequently, E_0 is an unstable node. Next, condition (2.3) at the semi-trivial equilibrium E_1 gives

$$\mathrm{Tr}(J)\Big|_{E_1} = -\alpha_2 + \frac{\alpha_1 c_2 + \alpha_2 c_1}{c_2}, \qquad \det(J)\Big|_{E_1} = -\alpha_1\alpha_2 - \frac{\alpha_2^2 c_1}{c_2}.$$

Because all parameters are positive, $\det(J)\Big|_{E_1} < 0$. Hence, the two eigenvalues have opposite signs, and E_1 is a saddle point.

At the second semi-trivial equilibrium E_2, we obtain

$$\mathrm{Tr}(J)\Big|_{E_2} = -\alpha_1 - \frac{\alpha_1\beta_2 - \alpha_2\beta_1}{\beta_1}, \qquad \det(J)\Big|_{E_2} = \alpha_1\left(\frac{\alpha_1\beta_2 - \alpha_2\beta_1}{\beta_1}\right).$$

Since $\alpha_2\beta_1 - \alpha_1\beta_2 > 0$, it follows that $\det(J)\Big|_{E_2} < 0$. Therefore, E_2 is also a saddle point. At the coexistence equilibrium E_3, the trace–determinant condition (2.3) gives

$$\mathrm{Tr}(J)\Big|_{E_3} = \frac{-\beta_1(\alpha_2 c_1 + \alpha_1 c_2) - c_2(\alpha_2\beta_1 - \alpha_1\beta_2)}{\beta_2 c_1 + \beta_1 c_2}, \qquad \det(J)\Big|_{E_3} = \frac{(\alpha_2\beta_1 - \alpha_1\beta_2)(\alpha_1 c_2 + \alpha_2 c_1)}{\beta_2 c_1 + \beta_1 c_2}.$$

Since all parameters are positive and $\alpha_2\beta_1 - \alpha_1\beta_2 > 0$, then $\mathrm{Tr}(J)\Big|_{E_3} < 0$ and $\det(J)\Big|_{E_3} > 0$. Therefore, the coexistence equilibrium E_3 is asymptotically stable. □

Lemma 5.1 establishes the baseline stability of the predator–prey system (5.4) in the absence of diffusion and advection. Under the condition $\frac{\alpha_2}{\alpha_1} > \frac{\beta_2}{\beta_1}$, the coexistence equilibrium E_3 exists and is asymptotically stable, whereas the extinction equilibrium E_0 is unstable and the boundary equilibria E_1 and E_2 are saddle points. Ecologically, this implies that neither extinction nor single-species persistence is a robust long-term state, while prey and predator can coexist stably. This stable kinetic setting is important because any instability that appears after incorporating diffusion, advection, cross-diffusion, or cross-advection can be interpreted as a transport-induced instability rather than an instability inherited from the local reaction dynamics.

By Theorem 3.6, stability under diffusion and advection requires that the corresponding equilibrium be stable in the spatially homogeneous system. Since Lemma 5.1 shows that E_0, E_1, and E_2 are linearly unstable, the RADCDCA stability analysis is restricted to the relevant equilibria E_3. Now, we investigate whether the instability induced by cross-diffusion and cross-advection occurs for the constant equilibrium solution E_3. We evaluate the elements of the Jacobian matrix J at E_3 under the assumption $\frac{\alpha_2}{\alpha_1} > \frac{\beta_2}{\beta_1}$ and obtain

$$\begin{aligned} F_u &= -\frac{\beta_1(\alpha_1 c_2 + \alpha_2 c_1)}{\beta_2 c_1 + \beta_1 c_2} < 0, \quad F_v = \frac{c_1(\alpha_1 c_2 + \alpha_2 c_1)}{\beta_2 c_1 + \beta_1 c_2} > 0, \\ G_u &= -\frac{\beta_2(\alpha_2\beta_1 - \alpha_1\beta_2)}{\beta_2 c_1 + \beta_1 c_2} < 0, \quad G_v = -\frac{c_2(\alpha_2\beta_1 - \alpha_1\beta_2)}{\beta_2 c_1 + \beta_1 c_2} < 0. \end{aligned} \tag{5.5}$$

For simplification, let us assume $y_1 = \frac{\alpha_1 c_2 + \alpha_2 c_1}{\beta_2 c_1 + \beta_1 c_2} > 0$ and $y_2 = \frac{\alpha_2 \beta_1 - \alpha_1 \beta_2}{\beta_2 c_1 + \beta_1 c_2} > 0$. By substituting F_u, F_v, G_u, and G_v in (5.5) into condition (3.21), we obtain

$$\Lambda_A - \frac{1}{4}\tau_A^2 + \tau_{DJ} = -y_a - (d_{22}\beta_1 + d_{21}c_1)y_1 - (d_{11}c_2 - d_{12}\beta_2)y_2. \tag{5.6}$$

where $y_a = a_{12}a_{21} + \frac{1}{4}(a_{11} - a_{22})^2 > 0$. From Theorem 3.6 and (5.6), we obtain the result summarized in the following theorem.

Theorem 5.2. *Let* $E_3 = \left(\frac{\alpha_1 c_2 + \alpha_2 c_1}{\beta_1 c_2 + \beta_2 c_1}, \frac{\alpha_2 \beta_1 - \alpha_1 \beta_2}{\beta_1 c_2 + \beta_2 c_1}\right)$ *be the positive constant equilibrium solution of RADCDCA system (5.1). Then, the following statements hold :*

1. *If* $\frac{\alpha_2}{\alpha_1} > \frac{\beta_2}{\beta_1}$, *then* E_3 *is asymptotically stable for the ODE system (5.4) and remains stable for the RAD system with* $d_{12} = d_{21} = a_{12} = a_{21} = 0$ *as well as for the RADCA system with* $d_{12} = d_{21} = 0$.
2. *If* $\frac{\alpha_2}{\alpha_1} > \frac{\beta_2}{\beta_1}$ *and* $\frac{d_{11}}{d_{12}} > \frac{\beta_2}{c_2}$, *then* E_3 *remains stable for the RADCDCA system (5.1) as well as RADCD system with* $a_{12} = a_{21} = 0$.

Based on Theorem 5.2, the equilibrium E_3 remains stable in the RAD, RADCD, and RADCA systems under the corresponding absence of cross-transport terms. This analytical result is further confirmed by the dispersion relation shown in Figure 7 with parameter values $d_{11} = d_{22} = 1$, $a_{11} = 0.2$, $a_{22} = 0.2$, $a_{12} = a_{21} = 0.1$, $d_{12} = d_{21} = 0.3$, $\alpha_1 = 0.2$, $\beta_1 = 0.2$, $c_1 = 0.3$, $\alpha_2 = 0.8$, $\beta_2 = 0.2$, and $c_2 = 0.6$. Figure 7 shows that all system configurations remain linearly stable, as $\mathrm{Re}(\lambda_{1,2}(k)) < 0$ for all k. The maximum value of $\mathrm{Re}(\lambda_{1,2}(k))$ is also negative, namely -0.55 for all RADCDCA, RADCD, RADCA, and RAD systems. Although $\mathrm{Re}(\lambda_{1,2}(k)) \neq 0$ appears in some scenarios, the oscillatory components remain damped because the real part of the eigenvalue is negative. Thus, there is no instability induced by self-diffusion, self-advection, cross-diffusion, or cross-advection in the parameters used.

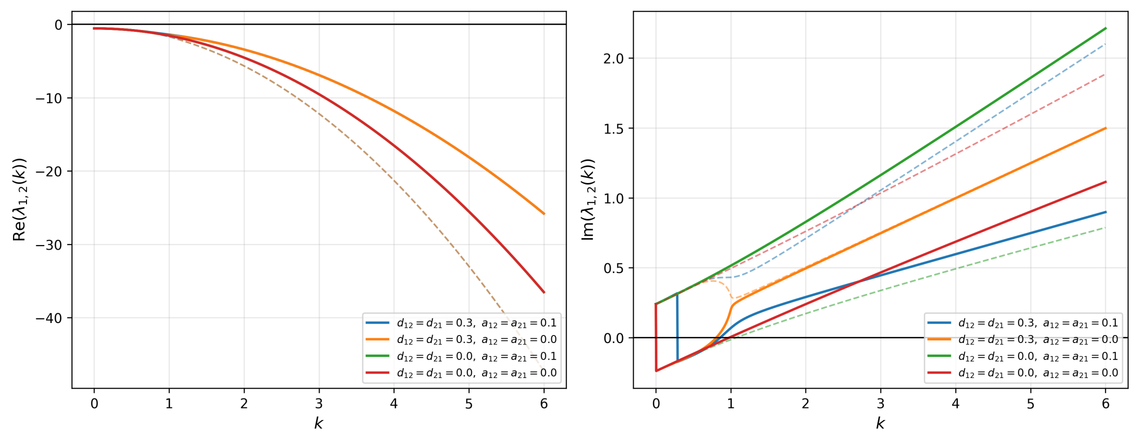

Figure 7. Plot of $\mathrm{Re}(\lambda_{1,2}(k))$ and $\mathrm{Im}(\lambda_{1,2}(k))$ under the assumptions $\alpha_2\beta_1 - \alpha_1\beta_2 = 0.12$ and $d_{11}c_2 - d_{12}\beta_2 = 0.54$.

For the case $\frac{d_{11}}{d_{12}} < \frac{\beta_2}{c_2}$, condition (3.22) in Theorem 3.6 can be positive if

$$(d_{12}\beta_2 - d_{11}c_2)y_2 > y_a + (d_{22}\beta_1 + d_{21}c_1)y_1. \tag{5.7}$$

Therefore, we need to reconsider whether this condition can trigger instability by examining condition (3.23). Next, we substitute (5.6) and (5.5) into condition (3.23) to obtain

$$\begin{aligned}(\Lambda_A - \frac{1}{4}\tau_A^2 + \tau_{DJ})^2 - 4\Lambda_D\Lambda_J =& \Big(- y_a - (d_{22}\beta_1 + d_{21}c_1)y_1 - (d_{11}c_2 - d_{12}\beta_2)y_2\Big)^2 \\ & - 4(\beta_1 c_2 + \beta_2 c_1)y_1 y_2(d_{11}d_{22} - d_{12}d_{21}).\end{aligned}$$

Considering that $\frac{d_{11}}{d_{12}} < \frac{\beta_2}{c_2}$, $y_a > 0$, and all parameters are positive, the condition $(\Lambda_A - \frac{1}{4}\tau_A^2 + \tau_{DJ})^2 - 4\Lambda_D\Lambda_J$ is positive if it satisfies

$$d_{21}c_2(d_{12}\beta_1 + d_{11}c_2) + d_{22}\beta_2(d_{11}c_1 - d_{12}\beta_1) + (d_{11}d_{22} - d_{12}d_{21})(\beta_2 c_1 - \beta_1 c_2) > \frac{y_a}{y_1}(d_{12}\beta_2 - d_{11}c_2). \quad (5.8)$$

Based on Theorem 4.11, we obtain the result in the following theorem.

Theorem 5.3. *If $\frac{\alpha_2}{\alpha_1} > \frac{\beta_2}{\beta_1}$, $\frac{d_{11}}{d_{12}} < \frac{\beta_2}{c_2}$, and conditions (5.7)–(5.8) are met, then the constant equilibrium solution E_3 is stable for the ODE system (5.4) but unstable for the RADCDCA system (5.1) and the RADCD system with $a_{12} = a_{21} = 0$.*

For the symmetric case where $d_{21} = d_{12}$ and $a_{21} = a_{12}$, conditions (5.7) and (5.8) become

$$d_{12} > \frac{r + d_{22}\beta_1 + sd_{11}c_2}{s\beta_2 - c_1} \quad (5.9)$$

with $s\beta_2 - c_1 > 0$ and

$$(2\beta_1 c_2 - \beta_2 c_1)d_{12}^2 + (d_{11}c_2^2 - d_{22}\beta_1\beta_2 - r\beta_2)d_{12} + d_{11}d_{22}(2\beta_2 c_1 - \beta_1 c_2) + rd_{11}c_2 > 0, \quad (5.10)$$

where $r = \frac{y_a}{y_1}$ and $s = \frac{y_2}{y_1}$. In this case, Theorem 5.3 can be expressed in a simpler form. This reduction provides practical criteria for observing the effects of cross-diffusion and cross-advection on instability in the constant equilibrium solution E_3. As a direct consequence of Theorem 5.3, the instability criteria can be simplified by assuming symmetric cross transport $d_{21} = d_{12}$ and $a_{21} = a_{12}$. This reduction yields the following corollary.

Corollary 5.4. *Assume that $d_{21} = d_{12}$, $a_{21} = a_{12}$, $\frac{\alpha_2}{\alpha_1} > \frac{\beta_2}{\beta_1}$, $\frac{d_{11}}{d_{12}} < \frac{\beta_2}{c_2}$, and conditions (5.9)-(5.10) hold. The constant equilibrium solution E_3 is stable for the ODE, RAD, and RADCA systems, but unstable for the RADCDCA and RADCD systems.*

Following the corollary, numerical validation is carried out by selecting positive parameters $a_{11} = a_{22} = 0.4$, $d_{11} = 0.5$, $d_{22} = 0.6$, $\alpha_1 = 0.05$, $\beta_1 = 0.1$, $c_1 = 0.05$, $\alpha_2 = 0.6$, $\beta_2 = 0.5$, and $c_2 = 0.1$ that ensure the existence of the positive equilibrium $E_3 = (1, 1)$. Using these parameters, the stability region predicted by Theorem 4.14 is visualized in the (a_{12}, d_{12})-plane as shown in Figure 8.

The Figure 8 shows that the combined effects of cross-diffusion and cross-advection on the stability of the positive equilibrium E_3 can be directly observed in the (a_{12}, d_{12})-plane. Region I identifies the instability domain, where certain combinations of a_{12} and d_{12} cause E_3 to lose stability through cross-transport interactions. In contrast, Regions II and III indicate stable domains, where small perturbations around E_3 decay over time. The boundary curves, including $a_{11}a_{22} - a_{12}^2 = 0$, $d_{11}d_{22} - d_{12}^2 = 0$, and the stability curve involving $\Lambda_A - \frac{1}{4}\tau_A^2 + \tau_{DJ} = 0$ and $(\Lambda_A - \frac{1}{4}\tau_A^2 + \tau_{DJ})^2 - 4\Lambda_D\Lambda_J = 0$, separate the stable and unstable parameter regimes. Thus, when the combined values of cross-advection a_{12} and cross-diffusion d_{12} enter Region I, the cross-transport mechanism becomes strong enough to induce instability in E_3. Conversely, parameters located in Regions II and III show that the combined cross-transport effects are still insufficient to destabilize the constant equilibrium solution.

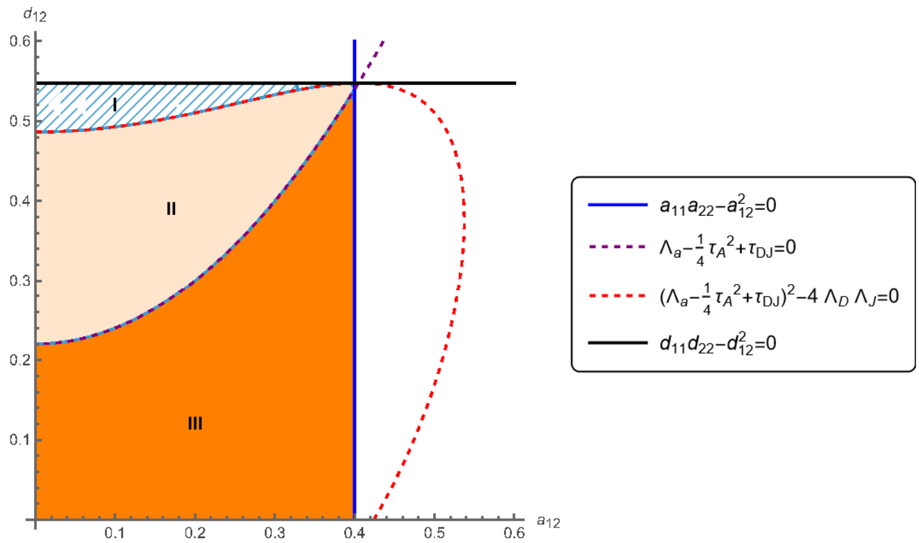

Figure 8. Parameter space for cross-diffusion- and cross-advection-driven instability. Region I denotes the instability domain, while Regions II and III represent stable domains.

To confirm this prediction, we select representative values of d_{12} and a_{12} from Region I in Figure 8, where the parameter-space analysis indicates the loss of stability of E_3. These values are then used to compute the dispersion relation $\lambda_{1,2}(k)$. As shown in Figure 9, instability appears only when cross-diffusion is sufficiently strong, namely when $d_{12} = d_{21} = 0.5$. In the left panel, the system becomes unstable for $a_{12} = a_{21} = 0.1$, with $k \in [0.570, 1.396]$ and $\max \mathrm{Re}(\lambda_{1,2}(k)) = 0.0245$, while the case without cross-advection remains unstable with $\max \mathrm{Re}(\lambda) = 0.0231$. In the right panel, increasing the cross-advection strength to $a_{12} = a_{21} = 0.35$ widens the unstable wavenumber interval to $k \in [0.305, 1.431]$ and increases the maximum growth rate to $\max \mathrm{Re}(\lambda_{1,2}(k)) = 0.0387$. By contrast, when $d_{12} = d_{21} = 0$, the system remains stable even in the presence of cross-advection. Therefore, cross-diffusion acts as the primary destabilizing mechanism, while cross-advection amplifies the instability and broadens the range of growing spatial modes.

To clarify the physical manifestation of the spectral instability, we next simulate the RADCDCA system using parameter values selected from the unstable regime. The analysis is formulated on the whole real line, whereas the numerical computations are performed on a sufficiently large finite interval subject to homogeneous Neumann (zero-flux) boundary conditions. This setting approximates the far-field regime of an open-flow aquatic environment, where spatial gradients are negligible at the artificial boundaries. We further verified that enlarging the computational domain does not alter the unstable wavenumber band, the selected wavelength, or the interior pattern profiles; boundary effects remain confined to narrow regions near the endpoints.

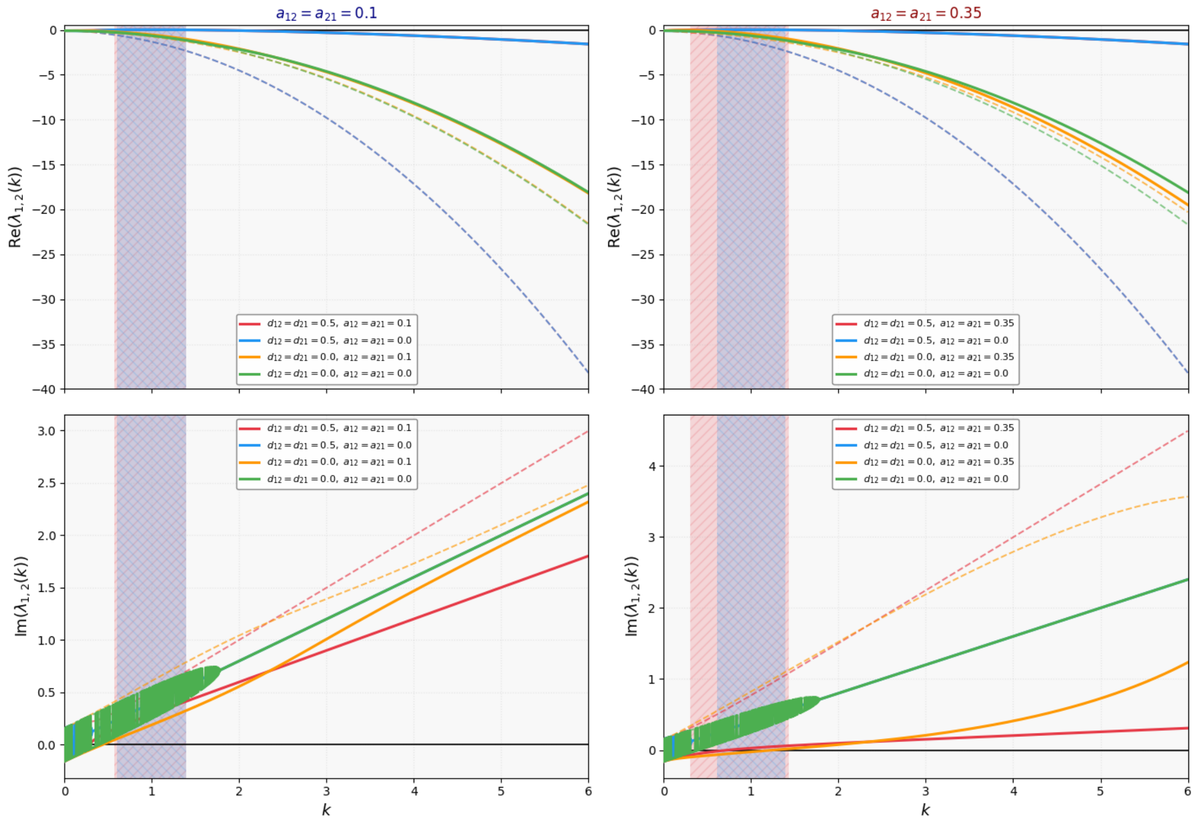

Figure 9. Effect of symmetric cross-diffusion and cross-advection on the dispersion relation $\mathrm{Re}(\lambda_{1,2}(k))$ and $\mathrm{Im}(\lambda_{1,2}(k))$.

Figure 10 display the spatiotemporal dynamics of $u(x,t)$ and $v(x,t)$ and show how small perturbations evolve into organized patterns. In the RAD and RADCA cases, where cross-diffusion is absent, the solution forms broad and smooth structures, indicating that cross-advection alone does not generate strong spatial patterning. By contrast, the RADCD case with $d_{12} = d_{21} = 0.5$ produces clear diagonal bands, which confirms that cross-diffusion drives the growth of spatial modes predicted by the dispersion relation. When cross-advection is added in the RADCDCA case, the patterns remain visible but become more directionally shifted and distorted, especially for the larger value $a_{12} = a_{21} = 0.35$. These results show that cross-diffusion provides the main mechanism for pattern formation, whereas cross-advection mainly changes the orientation, propagation, and intensity of the emerging wave-like structures.

Ecologically, this result shows that the predator–prey community can maintain a stable coexistence state E_3 as long as the cross-transport effects remain within the stable parameter regime. In this case, prey and predator densities tend to return to a homogeneous distribution after small spatial disturbances. However, when cross-transport becomes sufficiently strong, this coexistence state loses stability. The condition $\mathrm{Re}(\lambda_{1,2}(k)) > 0$ over a certain range of wavenumbers indicates that perturbations with specific spatial scales grow instead of decay. As a result, the population distribution no longer remains uniform and develops into spatiotemporal patterns. From an ecological viewpoint, cross-diffusion provides the main mechanism that initiates this spatial organization, since each species changes its distribution in response to the density gradient of the other. Cross-advection then strengthens this instability by introducing directed movement, such as prey avoidance and predator pursuit, which modifies the direction, intensity, and propagation of the emerging predator-prey patterns.

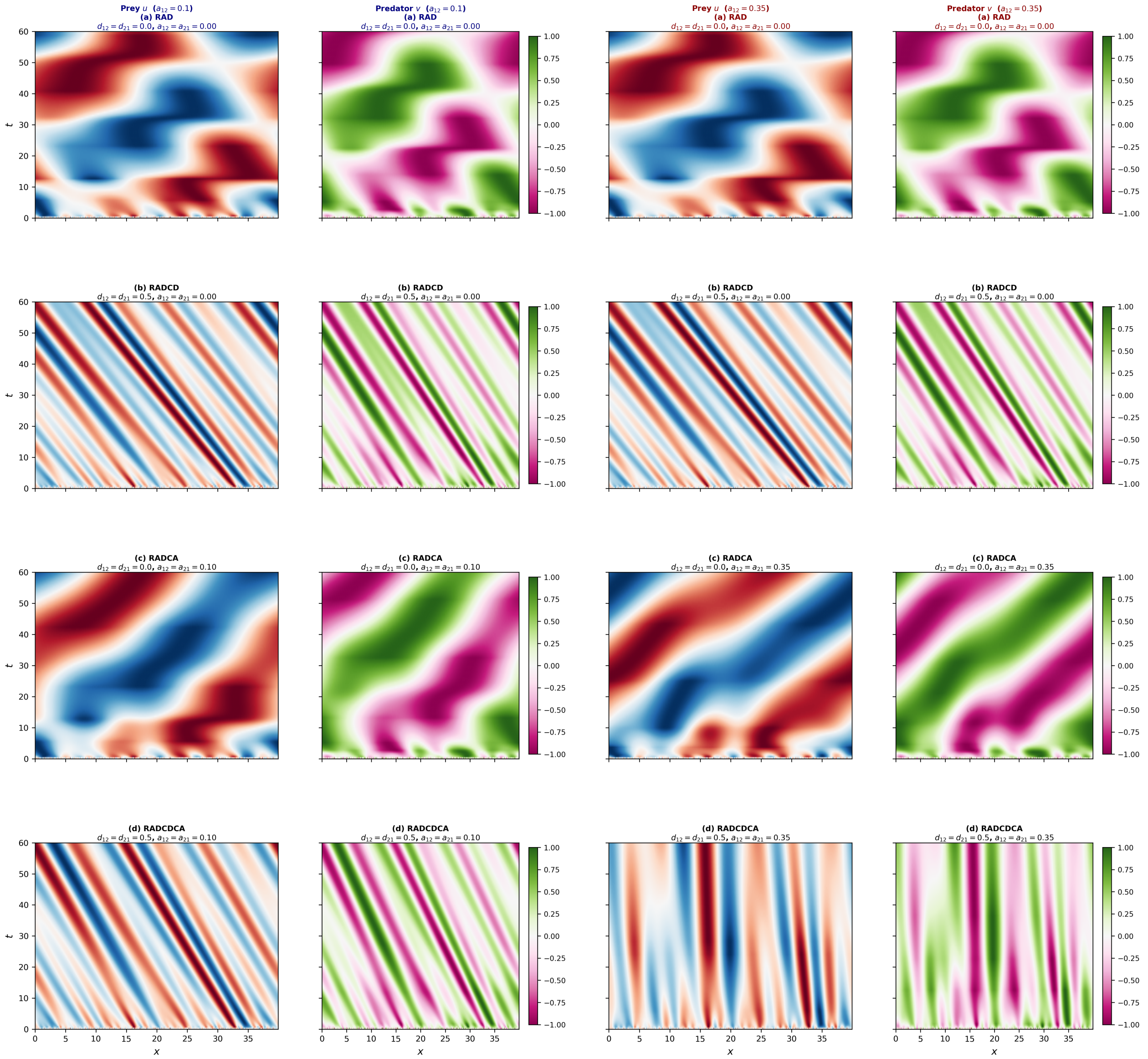

Figure 10. Spatiotemporal pattern formation of prey and predator populations driven by cross-diffusion and cross-advection.

6. Conclusions

This study established a general stability framework for reaction-advection-diffusion system with cross-diffusion and cross-advection on an infinite spatial domain. By considering general nonlinear reaction terms, the analysis was formulated in terms of the reaction Jacobian and transport matrices. Normal-mode decomposition, the Routh-Hurwitz criterion for complex characteristic polynomials, and the critical neutral curve method were used to derive stability criteria and to characterize the parameter regions where constant equilibria lose stability through cross-transport effects.

The results show that, under condition (A), a constant equilibrium that is stable for the local ODE system remains stable in the RAD and RADCA systems. Thus, self-diffusion, self-advection, and cross-advection alone do not destabilize the equilibrium in this setting. Cross-diffusion may destabilize the equilibrium when it acts alone in the RADCD system or interacts with cross-advection in the full RADCDCA system. Under conditions (B) and (C), asymmetric cross-advection may also induce instability in the RADCA system even without cross-diffusion. Therefore, the loss of stability identified in these cases arises from cross-transport mechanisms rather than from the local reaction dynamics.

The predator-prey application and numerical simulations support the analytical findings. The coexistence equilibrium remains stable when the transport parameters lie in the stable region, so small spatial disturbances decay and the populations return to a homogeneous coexistence state. When cross-transport becomes sufficiently strong, the dispersion relation admits unstable modes.This means that the associated eigenvalues possess a positive real part within a range of spatial wavenumbers. These unstable spectral modes then grow in time and organize into observable spatiotemporal patterns. In this setting, cross-diffusion acts as the main driver of spatial organization, while cross-advection strengthens and reshapes the emerging patterns by changing their direction, intensity, and propagation behavior. Overall, this work establishes a systematic framework for identifying instability induced by cross-transport mechanisms in generalized reaction-advection-diffusion systems.These findings may provide a useful foundation for future studies addressing bounded domains, higher-dimensional settings, nonlinear cross-transport effects, time delays, and convective-absolute instability classification.

Use of AI tools declaration

The authors declare they have not used Artificial Intelligence (AI) tools in the creation of this article.

Acknowledgement

The first author gratefully acknowledges financial support from the Indonesian Education Scholarship (BPI), Center for Higher Education Funding and Assesment (PPAPT), Ministry of Higher Education, Science, and Technology of Republic Indonesia, and Indonesian Endowment Fund for Education (LPDP) under grant number 01119/BPPT/BPI.06/9/2023. The authors also sincerely thank the anonymous reviewers for their careful evaluation and constructive comments, which have significantly improved the quality of this manuscript.

Conflict of interest

The authors declare no conflict of interest.

Author contributions

R. Setiyowati: Conceptualization, Methodology, Numerical Implementation, Investigation, Mathematical analysis, Writing original draft; L. Aryati: Supervision, Conceptualization, Methodology, Validation, Writing-review and editing; Sumardi: Supervision, Numerical analysis, Writing-review and editing; N. Susyanto: Supervision, Methodology, Visualization, Writing-review and editing. All authors have read and approved the final version of the manuscript.

References

1. H. Affan, R. Friedrich, Spiral defect chaos in an advection-reaction-diffusion system, *Phys. Rev. E*, **89** (2014), 1–8. https://doi.org/10.1103/PhysRevE.89.062920
2. W. Ao, J. Wei, M. Winter, Stable spikes for a reaction-diffusion system modeling color pattern formation, *Physica D*, **481** (2025), 134850. https://doi.org/10.1016/j.physd.2025.134850
3. D. L. Benson, J. A. Sherratt, P. K. Maini, Diffusion driven instability in an inhomogeneous domain, *Bull. Math. Biol.*, **55** (1993), 365–384. https://doi.org/10.1016/S0092-8240(05)80270-8
4. W. Choi, I. Ahn, Coexistence of two strongly competitive species in a reaction-advection-diffusion system, *Nonlinear Anal. RWA*, **81** (2025), 104187. https://doi.org/10.1016/j.nonrwa.2024.104187
5. J. Chung, Y. Kim, O. Kwon, C. Yoon, Biological advection and cross-diffusion with parameter regions, *AIMS Math.*, **4** (2019), 1721–1744. https://doi.org/10.3934/math.2019.6.1721
6. M. Crespo, B. Ivorra, A. M. Ramos, Asymtotic stability of a coupled advection-diffusion-reaction system arising in bioreactor processes, *Electron. J. Differ. Eq.*, **2017** (2017), 1–26.
7. B. Datsko, V. Gafiychuk, CMMMSE: New properties of auto-wave solutions in activator-inhibitor reaction-diffusion systems with fractional derivatives, *Math. Methods Appl. Sci.*, **48** (2025), 6292–6302. https://doi.org/10.1002/mma.10672
8. R. Feres, E. Pasewark, G. Yablonsky, Determination of output composition in reaction-advection-diffusion systems on network reactors, *Chem. Eng. Sci.*, **298** (2024), 1–26. https://doi.org/10.1016/j.ces.2024.120368
9. M. Fu, P. Liu, Q. Shi, Turing bifurcation in activator-inhibitor (depletion) models with cross-diffusion and nonlocal terms, *Stud. Appl. Math.*, **153** (2024), e12749. https://doi.org/10.1111/sapm.12749
10. W. Gan, Y. Shao, J. Wang, F. Xu, Global dynamics of a general competitive reaction-diffusion-advection system in one dimensional environments, *Nonlinear Anal. RWA*, **66** (2022), 103523. https://doi.org/10.1016/j.nonrwa.2022.103523
11. D. C. Guaca, E. Cristina, C. Poletti, Modeling and numerical simulation of dissolved oxygen and biochemical oxygen demand concentrations with Holling type III kinetic relationships, *Appl. Math. Comput.*, **415** (2022), 1–13. https://doi.org/10.1016/j.amc.2021.126690
12. D. Hinrichsen, A. J. Pritchard, *Mathematical Systems Theory I: Modelling, State Space Analysis, Stability and Robustness*, New York: Springer, 2000, 337–340. https://doi.org/10.1007/b137541
13. Y. Hori, H. Miyazako, Analysing diffusion and flow-driven instability using semidefinite programming, *J. R. Soc. Interface*, **16** (2019), 1–11. https://doi.org/10.1098/rsif.2018.0586

14. T. K. Kar, U. K. Pahari, S. Chaudhuri, Conservation of a prey-predator fishery with predator self limitation based on continous fishing effort, *JAMC*, **19** (1997), 311–326. https://doi.org/10.1007/BF02935807

15. K. Kawasaki, A. Mochizuki, M. matsushita, T. Umeda, N. Shigesada, Modeling spatiotemporal patterns generated by Bacillus subtilis, *J. Theor. Biol.*, **188** (2005), 177–185. https://doi.org/10.1006/jtbi.1997.0462

16. A. L. Krause, A. M. Burton, N. T. Fadai, R. A. Gorden, Emergent structures in reaction-advection-diffusion systems on a sphere, *Phys. Rev. E*, **97** (2018), 1–13. https://doi.org/10.1103/PhysRevE.97.042215

17. Y. Li, Y. Sun, J. Luo, J. Pang, B. Liu, Pattern formation mechanisms of spatiotemporally discrete activator-inhibitor model with self- and cross-diffusions, *Fractal Fract.*, **8** (2025), 1–26. https://doi.org/10.3390/fractalfract8120743

18. D. Liu, H. Wang, W. Jiang, Dynamics of a diffusion-advection lotka-volterra competition model with stage structure in a spatially heterogeneous environment, *J. Differ. Equations*, **372** (2023), 536–563. https://doi.org/10.1016/j.jde.2023.07.004

19. D. Luo, Q. Wang, L. Chen, Nonconstant steady states and pattern formations of generalized 1D cross-diffusion systems with prey-taxis, *Stud. Appl. Math.*, **150** (2023), 899–958. https://doi.org/10.1111/sapm.12560

20. L. Ma, Y. Feng, Stability and bifurcation in a two-species reaction-diffusion-advection competition model with time delay, *Nonlinear Anal. RWA*, **61** (2021), 103327. https://doi.org/10.1016/j.nonrwa.2021.103327

21. L. Ma, S. Guo, Bifurcation and stability of a two-species reaction-diffusion-advection competition model, *Nonlinear Anal. RWA*, **59** (2021), 103241. https://doi.org/10.1016/j.nonrwa.2020.103241

22. A. Madzvamuse, Stability analysis of reaction-diffusion systems with constant coefficients on growing domains, *Int. J. Dyn. Syst. Differ. Equ.*, **1** (2009), 250–262. https://doi.org/10.1504/IJDSDE.2008.023002

23. A. Madzvamuse, H. S. Ndakwo, R. Barreira, Cross-diffusion-driven instability for reaction-diffusion systems: Analysis and simulations, *J. Math. Biol.*, **70** (2015), 709–743. https://doi.org/10.1007/s00285-014-0779-6

24. Y. Maimaiti, W. Yang, Stability and pattern formation in a general class of reaction-diffusion-advection system, *Acta Appl. Math.*, **185** (2023), 1–23. https://doi.org/10.1007/s10440-023-00576-4

25. O. Medvedev, *Diffusion Coefficients in Multicomponent Mixtures*, Dissertation, Technical University of Denmark, 2005.

26. A. B. Medvinsky, S. V. Petrovskii, I. A. Tikhonova, H. Malchow, N. Li, Spatiotemporal complexity of plankton and fish dynamics, *SIAM Rev.*, **44** (2022), 311–370. https://doi.org/10.1137/S0036144502404442

27. R. Muolo, T. Carletti, H. Nakao, Cross-diffusion induced instability on networks, *J. Complex Netw.*, **12** (2024), cnad052. https://doi.org/10.1093/comnet/cnad052

28. A. J. Perumpanani, J. A. Sheratt, P. K. Maini, Phase differences in reaction-diffusion-advection systems and applications to morphogenesisis, *IMA J. Appl. Math.*, **55** (1995), 19–33. https://doi.org/10.1093/imamat/55.1.19
29. S. Petrovskii, B. Li, An exactly solvable model of population dynamics with density-dependent migrations and the allee effect, *Math. Biosci.*, **186** (2003), 79–91. https://doi.org/10.1016/S0025-5564(03)00098-1
30. B. Pimpunchat, W. L. Sweatman, G. C. Wake, W. Triampo, A. Parshotam, A mathematical model for pollution in a river and its remediation by aeration, *Appl. Math. Lett.*, **22** (2009), 304–308. https://doi.org/10.1016/j.aml.2008.03.026
31. H. Qiu, S. Guo, Bifurcation structures of a Leslie-Gower model with diffusion and advection, *Appl. Math. Lett.*, **135** (2023), 108391. https://doi.org/10.1016/j.aml.2022.108391
32. J. Shi, J. Xie, K. Little, Cross-diffusion induced instability and stability in reaction diffusion systems, *J. Appl. Anal. Comput.*, **1** (2011), 95–119. https://doi.org/10.11948/2011007
33. N. Shigesada, K. Kawasaki, E. Teramoto, Spatial segregation of interacting species, *J. Theoret. Biol.*, **79** (1979), 83–99. https://doi.org/10.1016/0022-5193(79)90258-3
34. E. Siero, A. Doelman, M. B. Eppingga, J. D. M. Rademacher, M. Rietkerk, M. Siteur, Pattern selection by advective reaction-diffusion systems: resilience of banded vegetation on slopes, *Chaos*, **25** (2015), 036411. https://doi.org/10.1063/1.4914450
35. V. K. Vanag, I. R. Epstein, Cross-diffusion and pattern formation in reaction-diffusion systems, *Phys. Chem. Chem. Phys.*, **11** (2009), 897–912. https://doi.org/10.1039/b813825g
36. W. Wang, G. Wu, X. Wang, Z. Feng, Dynamics of a reaction-advection-diffusion model for cholera transmission with human behavior change, *J. Differ. Equ.*, **373** (2023), 176–215. https://doi.org/10.1016/j.jde.2023.06.045
37. X. Wang, Y. Cai, Cross-diffusion-driven instability in a reaction-diffusion harrison predator-prey model, *Abstr. Appl. Anal.*, **2013** (2013), 306467. https://doi.org/10.1155/2013/306467
38. Y. Wang, Z. Ji, X. Li, Z. Long, Y. Pei, Comprehensive analysis of the migration and transformation of nutrients between sediment and overlying water in complex habitat systems, *Sci. Total Environ.*, **852** (2022), 158433. https://doi.org/10.1016/j.scitotenv.2022.158433
39. P. Wu, Y. Salmaniw, X. Wang, Threshold dynamics of a reaction-advection-diffusion schistosomiasis epidemic model with seasonality and spatial heterogeneity, *J. Math. Biol.*, **88** (2024), 76. https://doi.org/10.1007/s00285-024-02097-6
40. S. Xin, H. Nie, H. Shu, Joint impact of advection and diffusion on the predator-prey coexistence in an open flow, *Qual. Theory Dyn. Syst.*, **23** (2024), 290. https://doi.org/10.1007/s12346-024-01151-4
41. E. P. Zemskov, K. Kassner, M. A. Tsyganov, M. J. B. Hauser, Wavy fronts in reaction-diffusion systems with cross-advection, *Eur. Phys. J. B*, **72** (2009), 290. https://doi.org/10.1007/s12346-024-01151-4
42. E. P. Zemskov, M. A. Tsyganov, G. R. Ivanitsky, Solitary pulses and periodic wave trains in a bistable Fitzhugh-Nagumo model with cross-diffusion and cross-advection, *Phys. Rev. E*, **105** (2022), 014207. https://doi.org/10.1103/PhysRevE.105.014207

43. X. Zeng, Non-constant positive steady states of a prey-predator system with cross-diffusions, *J. Math. Anal. Appl.*, **332** (2007), 989–1009. https://doi.org/10.1016/j.jmaa.2006.10.075

44. T. Zhang, Yu Jin, Traveling waves for a reaction-diffusion-advection predator-prey model, *Nonlinear Anal. RWA*, **36** (2017), 203–232. https://doi.org/10.1016/j.nonrwa.2017.01.011

45. T. Zhang, Y. Xing, Bifurcation and stability of a reaction–diffusion–advection model with nonlocal delay effect and nonlinear boundary condition, *Nonlinear Anal. Real World Appl.*, **78** (2024), 104089. https://doi.org/10.1016/j.nonrwa.2024.104089

46. Y. Zheng, F. Yi, J. Wei, Cross-diffusion predator–prey model derived from behavioral states of predators, *Discrete Contin. Dyn. Syst. Ser. B*, **29** (2024), 3193–3216. https://doi.org/10.3934/dcdsb.2023098